C.2
Copy 6

NACA RM A53F16

RESEARCH MEMORANDUM

INVESTIGATION OF THE NACA 1.167-(0)(03)-058 AND NACA 1.167-(0)(05)-058 THREE-BLADE PROPELLERS AT FORWARD MACH NUMBERS TO 0.92 INCLUDING EFFECTS OF THRUST-AXIS INCLINATION

By Fred A. Demele and
William R. Otey

Ames Aeronautical Laboratory
Moffett Field, Calif.

CLASSIFICATION CHANGED
UNCLASSIFIED

NACA Research Abstracts
No. RN-116
effective
June 20, 1957
by authority of
at 7/9/57

CLASSIFIED DOCUMENT

This material contains information affecting the National Defense of the United States within the meaning of the espionage laws, Title 18, U.S.C., Secs. 793 and 794, the transmission or revelation of which in any manner to an unauthorized person is prohibited by law.

NATIONAL ADVISORY COMMITTEE
FOR AERONAUTICS

WASHINGTON
August 31, 1953

NASA Technical Library
3 1176 01438 6024

NACA RM A53F16

NATIONAL ADVISORY COMMITTEE FOR AERONAUTICS

RESEARCH MEMORANDUM

INVESTIGATION OF THE NACA 1.167-(0)(03)-058 AND NACA 1.167-(0)(05)-058 THREE-BLADE PROPELLERS AT FORWARD MACH NUMBERS TO 0.92 INCLUDING EFFECTS OF THRUST-AXIS INCLINATION

By Fred A. Demele and
William R. Otey

SUMMARY

An investigation has been made to determine the aerodynamic characteristics of the NACA 1.167-(0)(03)-058 and NACA 1.167-(0)(05)-058 three-blade propellers over a range of blade angles from -19° to 56° and through a Mach number range extending up to 0.92. Data were obtained at angles of thrust-axis inclination up to 16° for the thick-blade propeller, and up to 6° for the thin-blade propeller.

The results show that the thick-blade propeller was much more adversely affected by compressibility than was the thin-blade propeller; at the design forward Mach number of 0.83, the maximum efficiency of the thin-blade propeller was 75 percent as compared to 61 percent for the thick-blade propeller.

At the higher Mach numbers and propeller blade angles, there was generally a slight decrease in propeller thrust coefficient as a result of inclining the propeller to the air stream but the principal effect of inclination on propeller performance was a reduction in efficiency.

The variation of sea-level static thrust per horsepower with propeller-power disk loading was satisfactorily predicted by an actuator disk theory wherein only axial losses are considered. However, the experimental value of static thrust was about 65 percent of the theoretical ideal thrust.

INTRODUCTION

The supersonic propeller, in combination with the turbopropeller engine, constitutes a propulsive device which appears attractive for long-range airplanes operating at moderately high subsonic speeds.

CONFIDENTIAL

The experimental data on propellers designed specifically to operate at supersonic helical Mach numbers are meager, and few, if any, data are available to demonstrate the effects of propeller operation on the aerodynamic characteristics of an airplane at the large powers and high speeds associated with such an application.

The propeller investigation reported herein was undertaken as part of a more general investigation in the Ames 12-foot pressure wind tunnel of the effects of propeller operation on the longitudinal stability and control and on the performance of a model of a four-engine tractor airplane of a type believed suitable for long-range operation at high subsonic speeds. Because of the airplane model size and motor power limitations, the propellers investigated were of a smaller scale than desirable from the standpoint of propeller performance data. However, it was felt that the data could be utilized with reasonable accuracy and were of sufficient general interest to warrant separate publication.

The model propeller was a 1/12-scale model of a 14-foot, three-blade, supersonic-type propeller designed to absorb 5000 horsepower at an altitude of 40,000 feet and a Mach number of 0.83. The blade thickness-chord ratio at 0.70 radius was 0.03 and the activity factor was 188.4. A second propeller, identical to the first except for an increase in the thickness-chord ratio by a factor of 5/3, was designed specifically to withstand the very high blade loadings accompanying low-speed, high-density, wind-tunnel operation.

Presented herein are results of force tests of these propellers over a range of blade angles from -19° to 56° and through a Mach number range extending up to 0.92. Results were obtained at angles of thrust-axis inclination up to 6° for the thin-blade propeller, and up to 16° for the thick-blade propeller. The static-thrust characteristics of both propellers were also investigated and the thicker propeller was tested at low speeds under conditions of negative thrust.

NOTATION

A upflow angle, angle of local flow at 0.7 propeller radius and at the horizontal center line of the propeller plane, measured with respect to the thrust axis in a plane parallel to the nacelle plane of symmetry, deg

b blade width, ft

C_P power coefficient, $\frac{P}{\rho n^3 D^5}$

C_T thrust coefficient, $\frac{T}{\rho n^2 D^4}$

D propeller diameter, ft

$\frac{b}{D}$ blade width ratio

h maximum thickness of blade section, ft

h_o tunnel pressure, psia

HP power, horsepower

$\frac{h}{b}$ blade thickness ratio

J advance ratio, $\frac{V}{nD}$

M free-stream Mach number

M_t helical-tip Mach number, $M\sqrt{1 + \left(\frac{\pi}{J}\right)^2}$

n propeller rotational speed, rps

P power, ft-lb/sec

q free-stream dynamic pressure, $\frac{\rho V^2}{2}$, lb/sq ft

r blade-section radius, ft

R Reynolds number per foot, $\frac{\rho V}{\mu}$

R_t propeller-tip radius, ft

S propeller disk area, sq ft

T thrust, measured parallel to free stream, lb

T_c thrust disk-loading coefficient, $\frac{T}{\rho V^2 D^2}$

V free-stream velocity, ft/sec

α angle of attack of the thrust axis, measured with respect to the free-stream direction, deg

β' section blade angle, deg

β section blade angle at 0.7 radius, deg

η efficiency, $\frac{C_T}{C_P} J$

η_{max} maximum efficiency

ρ air density, slugs/cu ft

MODEL AND APPARATUS

This investigation was conducted in the Ames 12-foot pressure wind tunnel, which is a closed-throat variable-density wind tunnel having a low turbulence level closely approximating that of free air. The nacelle assembly was mounted on the tunnel semispan-model support system located in the floor of the test section. Hence, rotation of the supporting turntable permitted inclination of the thrust axis to the air stream. A photograph of the assembly mounted in the tunnel is shown in figure 1, and a schematic drawing of the assembly is shown in figure 2. Coordinates of the body portion of the assembly are given in table I.

Nacelle Assembly

The primary structure of the nacelle assembly consisted of an electric motor and integral gearbox supported by a strut rigidly mounted to the framework of the six-component balance system. The secondary structure consisted of a fairing enclosing the after portion of the motor and the support strut. This fairing was rigidly attached to the wind-tunnel-floor structure and was independent of the primary structure attached to the balance system. The fairing had no influence on the measured propeller forces other than its unknown effect on the flow field in the region of the propeller. A clearance gap was provided between the primary and secondary nacelle structure as shown in figure 2 to prevent transmission of extraneous forces to the balance system. The region behind the clearance gap was sealed with a concentric rubber membrane, and static-pressure orifices were provided on either side of the seal in order to determine the pressure forces acting on the rear of the primary nacelle structure.

Power Transmission Unit

The propeller was driven through gears by a constant-torque electric motor having a normal rating of 75 horsepower at 18,000 revolutions per minute. Continuous speed control of the motor was accomplished by means of a variable-frequency power supply. Motor-speed indication was provided by a frequency-measuring instrument connected to a four-pole variable-reluctance alternator located on the rear of the motor. The ratio of propeller speed to motor speed was either 1.5 to 1 or 1 to 1.5, depending on the arrangement of the gears in the gearbox.

Spinner

The spinner used in this investigation had a maximum diameter of 4.20 inches and the NACA 1-series profile. The diameter at the plane of the propeller was 3.97 inches, or 28.3 percent of the propeller diameter, and the length forward of the propeller plane was 5.00 inches. Coordinates of the spinner are given in table I. A clearance gap of 0.015 inch was provided between the spinner and the forward face of the power transmission unit. Individual spinners were provided with blade cutouts corresponding to each blade angle.

Propellers

The NACA 1.167-(0)(03)-058 three-blade propeller was a 1/12-scale model of a propeller designed to absorb 5000 horsepower with an efficiency of 75 percent at a forward Mach number of 0.83 and an altitude of 40,000 feet. The design value of advance ratio was 2.01 and the design blade angle at 0.70 radius was 46.3°.

The NACA number designation of the 1.167-(0)(03)-058 propeller indicates a diameter of 1.167 feet and the following design characteristics at 0.70 radius: section design lift coefficient, 0; thickness-chord ratio, 0.03; and solidity per blade, 0.058. The propeller had an activity factor of 188.4 per blade. The NACA 16-series symmetrical airfoil was used for the blade sections.

For the twist distribution used, calculations indicated that the sections of the blade would operate at lift coefficients generally above those for maximum section lift-drag ratio at the design condition. Designs were considered in which all blade sections operated at maximum lift-drag ratio. In all these cases, either the solidity was felt to be excessive or the diameter was too large to install conveniently on the assumed airplane. It was felt that the small penalty in performance

resulting from overloading the propeller was justified in view of the practical difficulties and weight penalties associated with the larger propeller. The inner portions of the blades were modified slightly to allow for the increased velocity field of the spinner. Allowances were made for the change of twist of the blade due to aerodynamic and centrifugal forces at the design condition.

The blade plan form and the radial distribution of blade thickness were selected from considerations of propeller efficiency, blade stresses, 1 × P (once per revolution) resonance, and stall flutter. Check calculations, performed by the Propeller Division of the Curtiss-Wright Corporation, indicated that the rpm for 1 × P resonance at a blade angle of 46° was 38,000 (compared to the maximum operating rpm of 27,000), and that stall flutter should not occur within the operating range of the propeller.

The NACA 1.167-(0)(05)-058 propeller was identical to the NACA 1.167-(0)(03)-058 propeller except that the blade thicknesses were increased by a factor of 5/3 at all radial stations. These thicker blades were designed to withstand the very high blade loadings accompanying low-speed operations in the wind tunnel at an air density of 6 atmospheres.

All propeller blades used in this investigation were machined from heat-treated alloy steel. A photograph of the blades is shown in figure 3, and blade-form curves are presented in figure 4.

TEST CONDITIONS

Thrust, power, and rotational speed were measured for both the NACA 1.167-(0)(03)-058 and the NACA 1.167-(0)(05)-058 propellers for various blade angles at several angles of inclination, Mach numbers, and Reynolds numbers. Propeller rotational speeds were varied for a given blade angle at each Mach number, Reynolds number, and angle of inclination to obtain the data. The range of conditions investigated is shown in table II.

REDUCTION OF DATA

Propeller Thrust

Propeller thrust as used herein is the difference between the longitudinal force produced by the propeller-spinner combination and nacelle forebody (i.e., that portion forward of nacelle station 21.30

(see table I)) and the longitudinal force produced by the spinner and nacelle forebody in the absence of the propeller at the same Mach number and Reynolds number. The longitudinal force was measured by the six-component balance system.

Power

In order to determine the power absorbed by the propeller, the motor and gearbox were calibrated in the absence of the propeller throughout the range of rotational speeds and torques utilized during the investigation. Calibrations were made prior to and during the tests. No torque correction was applied for spinner skin friction as it amounted to a negligible percentage of the combined power loss.

Seal-pressure correction.- The pressures acting on the rear face of the power transmission unit were measured by pressure tubes located ahead of and behind the pressure seal. These pressure forces were adjusted for computational purposes to correspond to a base pressure equal to the free-stream static pressure. The component of this pressure force in the streamwise direction was added to the measured thrust for tests with the propeller operating and also with the propeller removed. Choice of free-stream static pressure for a reference pressure determined the net tare force but had no effect on the propeller thrust as defined herein.

Tunnel-wall correction.- The data have been corrected for the effect of tunnel-wall constraint on the velocity in the region of the propeller plane by the method of reference 1. The calculations were made for that portion of the nacelle forward of the nacelle-strut intersection. The nacelle structure aft of the nacelle-strut intersection was considered to have little or no effect upon tunnel-wall constraint in the region of the propeller plane and was omitted in the calculation. The magnitude of the maximum correction applied to the data was 0.7 percent. The constriction effects due to operating the propeller were evaluated by the method of references 2 and 3 and were found to be negligible.

Accuracy of results.- Analysis of the sources of error and correlation of duplicate test data indicate the probable maximum error in the accompanying data is as follows:

η, percent	C_T, percent	C_P, percent	J, percent	β, deg
±1.5	±1.5	±1.5	±0.5	±0.15

At power conditions close to zero, the error in efficiency and thrust and power coefficients, may be considerably greater than the tabulated values.

RESULTS

The results of this investigation are presented graphically in figures 5 through 23. Table II is an index of these figures and indicates the range of variables shown in each figure. Presented in figures 5 through 12 are the basic propeller characteristics for various Mach numbers and Reynolds numbers. The effects of Mach number on maximum efficiency are summarized in figures 13 through 15. Cross plots of the data in figures 5 through 8 are presented in figures 16 through 18 to show the effects of thrust-axis inclination on propeller performance. The negative-thrust characteristics are presented in figures 19 and 20, and the static-thrust characteristics are presented in figures 21 through 23.

DISCUSSION

Because of the lack of experimental data on propellers designed to operate at supersonic helical Mach numbers, a comparison of the measured and predicted characteristics at the design conditions was considered noteworthy. The following table compares the design characteristics for the full-scale propeller ($M = 0.83$; $D = 14$ ft; altitude = 40,000 ft) with measured characteristics of the NACA 1.167-(0)(03)-058 propeller, obtained by interpolation and by minor extrapolation of the data presented in figure 5(d):

Characteristics	Conditions			
	Design	A	B	C
HP	5000	5000	5000	3000
η, percent	75	69	70	75
J	2.01	2.01	1.80	1.94
β, deg	46.3	47.6	44.0	44.0

It may be noted for condition A that to absorb 5000 horsepower at the design value of advance ratio, the experimental efficiency was 69 percent compared to the design value of 75 percent. By altering the advance ratio and blade angle, the design horsepower was obtained with an efficiency of 70 percent (condition B). It is shown under condition C that for the design efficiency of 75 percent, only 3000 horsepower could be absorbed.

Effects of Mach Number

The effects of Mach number on the aerodynamic characteristics of the NACA 1.167-(0)(03)-058 propeller are shown in figures 5 through 7. The maximum efficiency in figure 5 is presented as a function of forward Mach number in figure 13. The maximum efficiency varied from 81 percent at a Mach number of 0.60 to 65 percent at a Mach number of 0.92. In general, the absolute magnitude of maximum efficiency varied less than 2 percent as a consequence of changing blade angle from 41° to 56°. It will be shown subsequently that maximum efficiency increased with increasing Reynolds number above a Mach number of 0.83; hence, for the full-scale propeller, higher efficiencies than those indicated herein may possibly be achieved at the higher Mach numbers.

Figure 14, which presents the variation of maximum efficiency with tip Mach number, indicates that as blade angle increased, there was a decrease in the tip Mach number at which maximum efficiency began to decrease rapidly. This was due, in part, to the fact that for a given tip Mach number, increasing the blade angle required an increase in the advance ratio and forward Mach number for maximum efficiency, which decreased the helical Mach number gradient along the blade. A greater portion of the blade was therefore exposed to the adverse effects of compressibility.

The variation of maximum efficiency with advance ratio for Mach numbers from 0.60 to 0.92 may be seen in figure 15, which indicates relative insensitivity of maximum efficiency to advance ratio over the entire Mach number range. Similar results have been previously reported (ref. 4) for a supersonic-type propeller operating at supersonic tip speeds for the same range of advance ratios covered in this investigation.

The effects of small changes in Mach number on the low-speed characteristics of the thick-blade propeller were small as shown in figures 8 and 9. The maximum tip Mach number in these cases was less than 0.7. At higher forward speeds and tip Mach numbers greater than 1.0, the effects of Mach number became much more pronounced, as shown in figure 12. It is also apparent from figure 12 that the thick-blade propeller was much more adversely affected by Mach number than was the thin-blade propeller. For example, at an advance ratio of 2.0, increasing the

Mach number from 0.60 to 0.83 resulted in a decrease in efficiency of about 16 percent for the thick-blade propeller as compared to about 6 percent for the thin-blade propeller. At a forward Mach number of 0.83, the efficiency of the thin-blade propeller was 75 percent as compared to about 60 percent for the thick-blade propeller.

Effects of Reynolds Number

The data in figure 10 indicate that changing the Reynolds number from 800,000 to 1,600,000 altered the basic characteristics of the thin-blade propeller only slightly below a Mach number of 0.83. Above this Mach number, the maximum efficiency was increased from 3 to 5 percent. At a Mach number of 0.90 (fig. 10(b)) there was generally a considerable difference between the data at the two different Reynolds numbers at any given value of advance ratio. It should be noted that a part of this difference is attributable to a small error in blade-angle setting in addition to any effect of Reynolds number on either the aerodynamic or aeroelastic properties of the blades.

Effects of Inclination

The data in this section are presented in terms of the upflow angle measured at 0.7 propeller radius in order to show a more realistic flow angle than that indicated by the angle of attack of the thrust axis. The angle of upflow at the propeller disk differs from the geometric angle of attack of the thrust axis by the amount of the upwash induced by the spinner and the nacelle. The upflow angles for the present spinner-nacelle combination have been measured and were reported in reference 5.

Basic characteristics.- The data presented in figures 16 and 17, which are cross plots of the data presented in figures 5 through 8, show the effect of inclination of the thrust axis on the characteristics of the thick- and thin-blade propellers, respectively. For the range of blade angles from 21° to 31° (thick-blade propeller), the efficiency decreased due to an increase in the power coefficient with increasing angle of inclination, while the thrust coefficient was relatively unaffected by inclination. At the highest blade angle (β = 36°), the thrust coefficient decreased as the angle of inclination increased while the power coefficient increased, resulting in a reduction in efficiency. In contrast, at higher forward speeds and blade angles (thin-blade propeller) there was essentially no change in the power coefficient with angle of inclination, but the efficiency decreased due to a decrease in the thrust coefficient.

Maximum efficiency.- The effects of blade angle and of inclination of the thrust axis on the maximum efficiency of the thick-blade propeller at a Mach number of 0.123 are shown in figure 18. At low angles of inclination, the efficiency was increased approximately 10 percent as the blade angle was increased from 21° to 36°; however, this gain in efficiency was reduced to essentially zero at an angle of inclination of 16°.

Negative-Thrust Characteristics

The basic characteristics of the thick-blade propeller in negative thrust are presented in figure 19 and have been plotted as a function of blade angle in figure 20. It may be noted that at the higher advance ratios, relatively constant negative-thrust coefficient was attained for a range of blade angles from -5° to -19°, and reached a maximum value at about -14°. Beyond -14° the negative-thrust coefficient decreased. However, the power coefficients corresponding to this range of blade angles increased rapidly, indicating that an increase in negative blade angle resulted in additional power absorption rather than in thrust.

Static-Thrust Characteristics

In figures 21 and 22 propeller static-thrust characteristics are presented as a function of the product of rotational speed and the diameter. A comparison of the thick- and thin-blade characteristics (fig. 22) indicates that both the thrust and power coefficients were higher for the thin-blade propeller at the higher rotational speeds. Upon consideration of the probable differences in the aeroelastic deformation of the two propellers, it is concluded that the thin blades were operating at effectively higher blade angles.

The experimental and theoretical static thrust per horsepower is presented in figure 23 as a function of power disk loading. These experimental values were calculated with the use of the data in figure 21 for a tunnel pressure of 3.5 pounds per square inch absolute, by obtaining the variation of static thrust per horsepower with power disk loading for constant values of nD. These latter data form a series of curves of which the experimental curve shown in figure 23 is the envelope. The theoretical ideal thrust per horsepower was computed by the method of reference 6. The variation of static thrust per horsepower with disk loading was similar for both theory and experiment; however, the experimental values were approximately 65 percent of the theoretical ideal values. This difference between theory and experiment is presumably due to rotational losses and blade drag, which were neglected in the theory.

CONCLUDING REMARKS

Results of tests conducted on the NACA 1.167-(0)(03)-058 and NACA 1.167-(0)(05)-058 three-blade propellers for blade angles from -19° to 56° throughout a Mach number range extending up to 0.92 show the following:

1. At the design forward Mach number of 0.83, the maximum efficiency of the thin-blade propeller was 75 percent as compared to 61 percent for the thick-blade propeller.

2. The principal effect on propeller performance of inclining the propellers to the air stream was a reduction in efficiency.

3. At the higher advance ratios, relatively constant negative thrust coefficient was attained for a range of blade angles from -5° to -19°. The corresponding power coefficients increased rapidly with increasing negative blade angle.

4. The static thrust of the propeller varied with power disk loading in the manner predicted by actuator disk theory. However, the experimental static thrust was about 65 percent of the theoretical ideal thrust.

Ames Aeronautical Laboratory
National Advisory Committee for Aeronautics
Moffett Field, Calif., June 16, 1953

REFERENCES

1. Herriot, John G.: Blockage Corrections for Three-Dimensional-Flow Closed-Throat Wind Tunnels, With Consideration of the Effect of Compressibility. NACA Rep. 995, 1950.(Formerly NACA RM A7B28)

2. Glauert, H.: The Elements of Aerofoil and Airscrew Theory. American Ed., The Macmillan Company, N. Y., 1943, pp. 222-226.

3. Young, A. D.: Note on the Application of the Linear Perturbation Theory to Determine the Effect of Compressibility on the Wind Tunnel Constraint on a Propeller. RAE TN No. Aero 1539, Nov. 1944.

4. Evans, Albert J., and Liner, George: A Wind-Tunnel Investigation of the Aerodynamic Characteristics of a Full-Scale Supersonic-Type Three-Blade Propeller at Mach numbers to 0.96. NACA RM L53F01, 1953

5. Lopez, Armando E., and Dickson, Jerald K.: The Effects of Compressibility on the Upwash at the Propeller Planes of a Four-Engine Tractor Airplane Configuration Having a Wing With 40° of Sweepback and an Aspect Ratio of 10. NACA RM A53A30a, 1953.

6. Gilman, Jean, Jr.: Analytical Study of Static and Low-Speed Performance of Thin Propellers Using Two-Speed Gear Ratios to Obtain Optimum Rotational Speeds. NACA RM L52I09, 1952.

TABLE I.- COORDINATES OF NACELLE ASSEMBLY

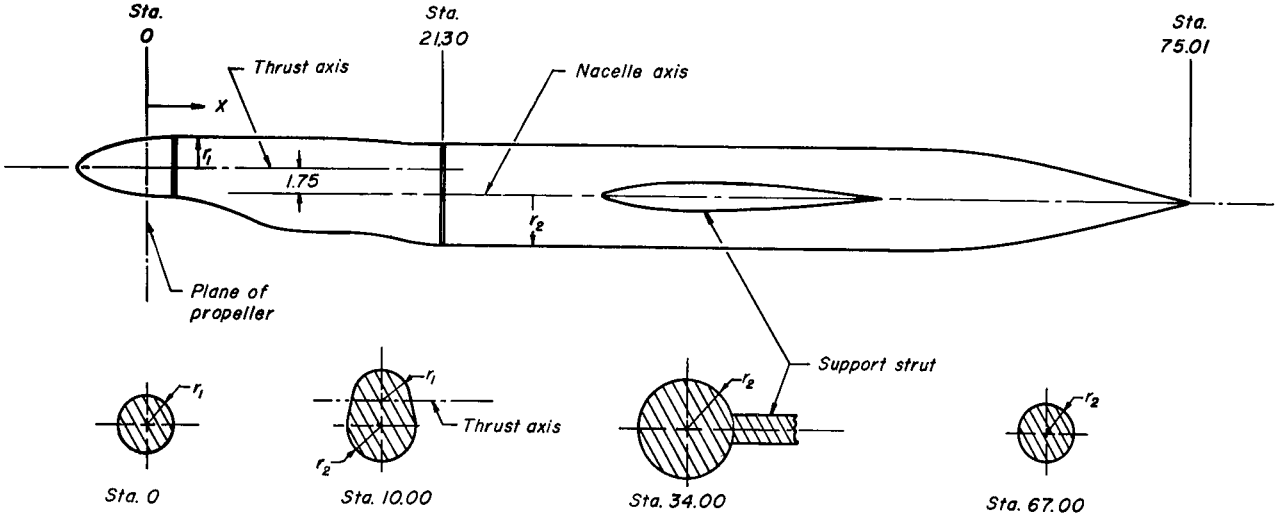

Distance from propeller plane x	Radius from thrust axis r_1	Distance from propeller plane x	Radius from thrust axis r_1	Radius from nacelle axis r_2	Distance from propeller plane x	Radius from thrust axis r_1	Radius from nacelle axis r_2	Distance from propeller plane x	Radius from nacelle axis r_2
-5.00	0	2.00	2.100	0.350	13.00	2.083	2.641	57.60	3.39
-4.79	.385	3.00	↓	.419	14.00	2.047	2.703	59.60	3.25
-4.58	.567	4.00		.616	15.00	1.969	2.781	61.60	3.04
-4.25	.788	5.00		.919	16.00	1.891	2.891	63.60	2.74
-3.95	.951	6.00		1.290	17.00	1.823	3.016	65.60	2.36
-3.25	1.242	7.00		1.685	18.00	1.797	3.141	67.60	1.91
-2.55	1.472	8.00		2.056	19.00	1.766	3.297	69.60	1.41
-1.80	1.670	9.00		2.359	20.00	1.750	3.422	71.60	.91
-.80	1.871	10.00		2.556	21.00	1.750	3.500	73.60	.38
0	1.985	11.00		2.625	53.60		3.500	75.01	0
		12.00		2.625	55.60		3.470		

All dimensions are in inches unless otherwise noted.

TABLE II.- INDEX OF DATA FIGURES

Figure number	Plot	Mach number, M	Reynolds number per ft, $R \times 10^{-6}$	Angle of attack, α, deg	Blade angle, β deg	Propeller
5	$C_T, C_P, \eta,$ M_t vs J	0.60 to 0.92	1.6	0	41,46, 51,56	thin
6	↓	0.60 to 0.92	↓	4	↓	↓
7	↓	0.60 to 0.80	↓	6	↓	↓
8	↓	0.082,0.123	3.2	0 to 16	21,26, 31,36	thick
9	↓	0.082,0.123, 0.165	↓	0	↓	↓
10	↓	0.80 to 0.90	0.8,1.6	↓	51	thin
11	↓	0.123, 0.165	3.2 to 6.4	↓	21,26, 31,36	thick
12	↓	0.60 to 0.83	1.6	↓	46	thick and thin
13	η_{max} vs M	0.60 to 0.92	↓	↓	41,46, 51,56	thin
14	η_{max} vs M_t	----------	↓	↓	↓	↓
15	η_{max} vs J	0.60 to 0.92	↓	↓	↓	↓
16	$C_T, C_P,$ η vs A	0.123	3.2	------	21,26, 31,36	thick
17	↓	0.60 to 0.80	1.6	------	46	thin
18	η_{max} vs β	0.123	3.2	------	21 to 36	thick
19	(a) C_T vs J (b) C_P vs J	0.082	3.2	0	-19 to 26	thick
20	(a) C_T vs β (b) C_P vs β	↓	↓	↓	↓	↓
21	C_T, C_P vs nD	0	0	↓	11,16,21	↓
22	↓	↓	↓	↓	11,16	thick and thin
23	T/HP vs HP/S	↓	↓	↓	11 to 21	thick

NACA

Figure 1.- Photograph of the nacelle assembly.

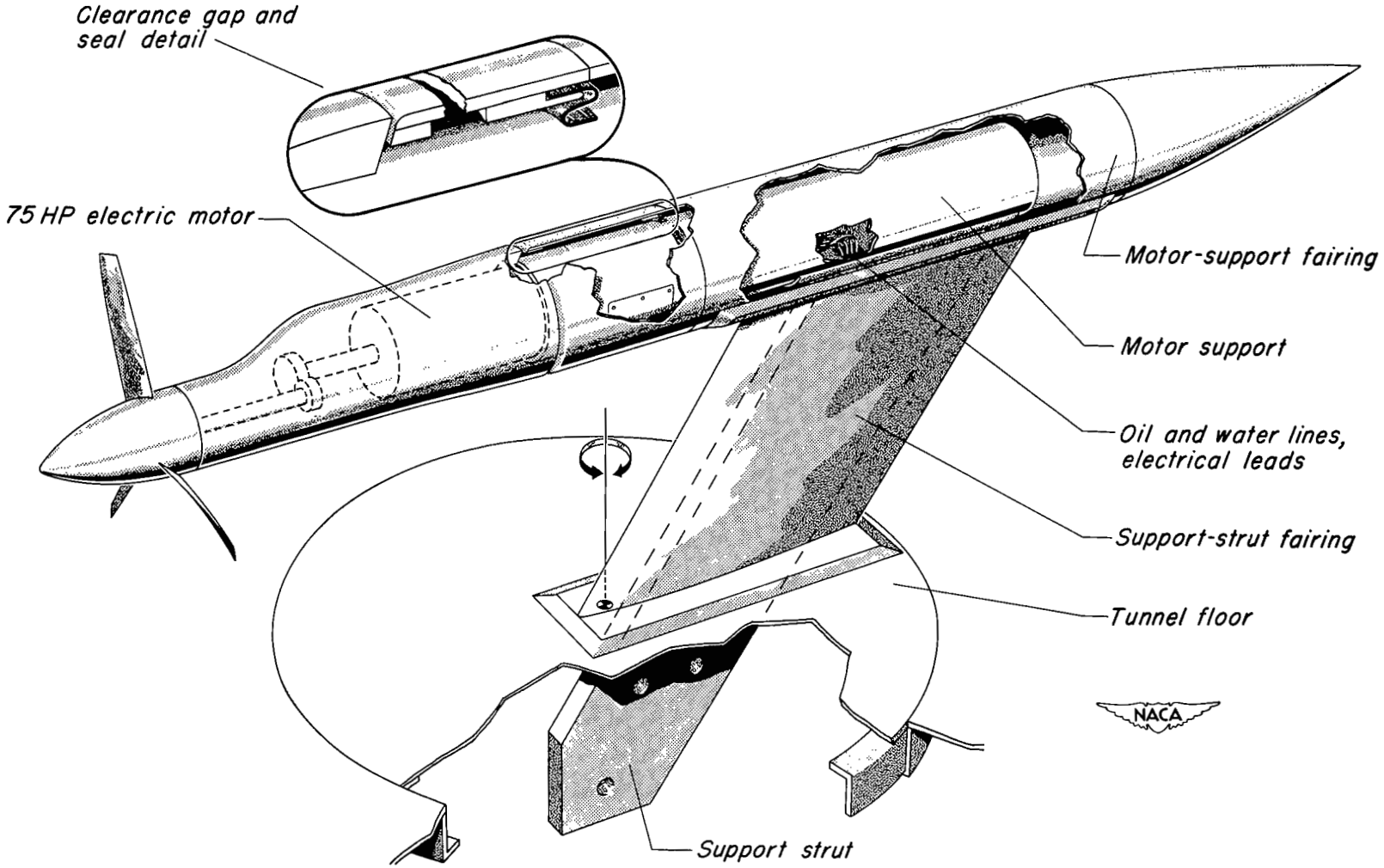

Figure 2.- Nacelle assembly.

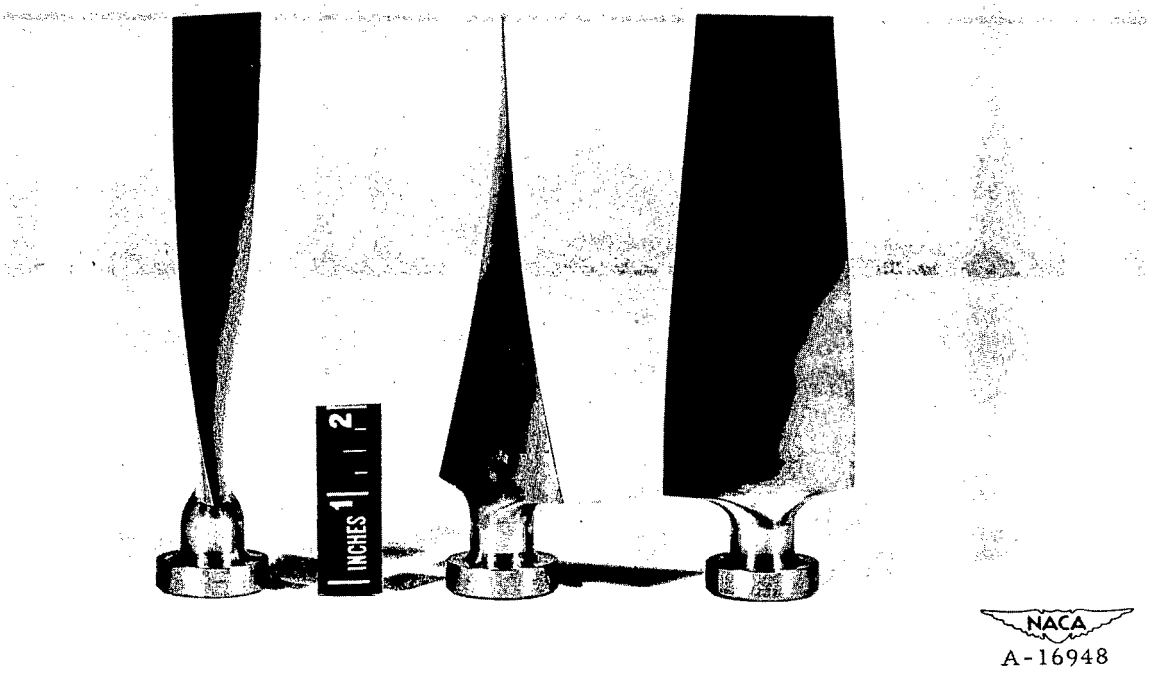

Figure 3.- Photograph of the NACA 1.167-(0)(03)-058 model propeller blades.

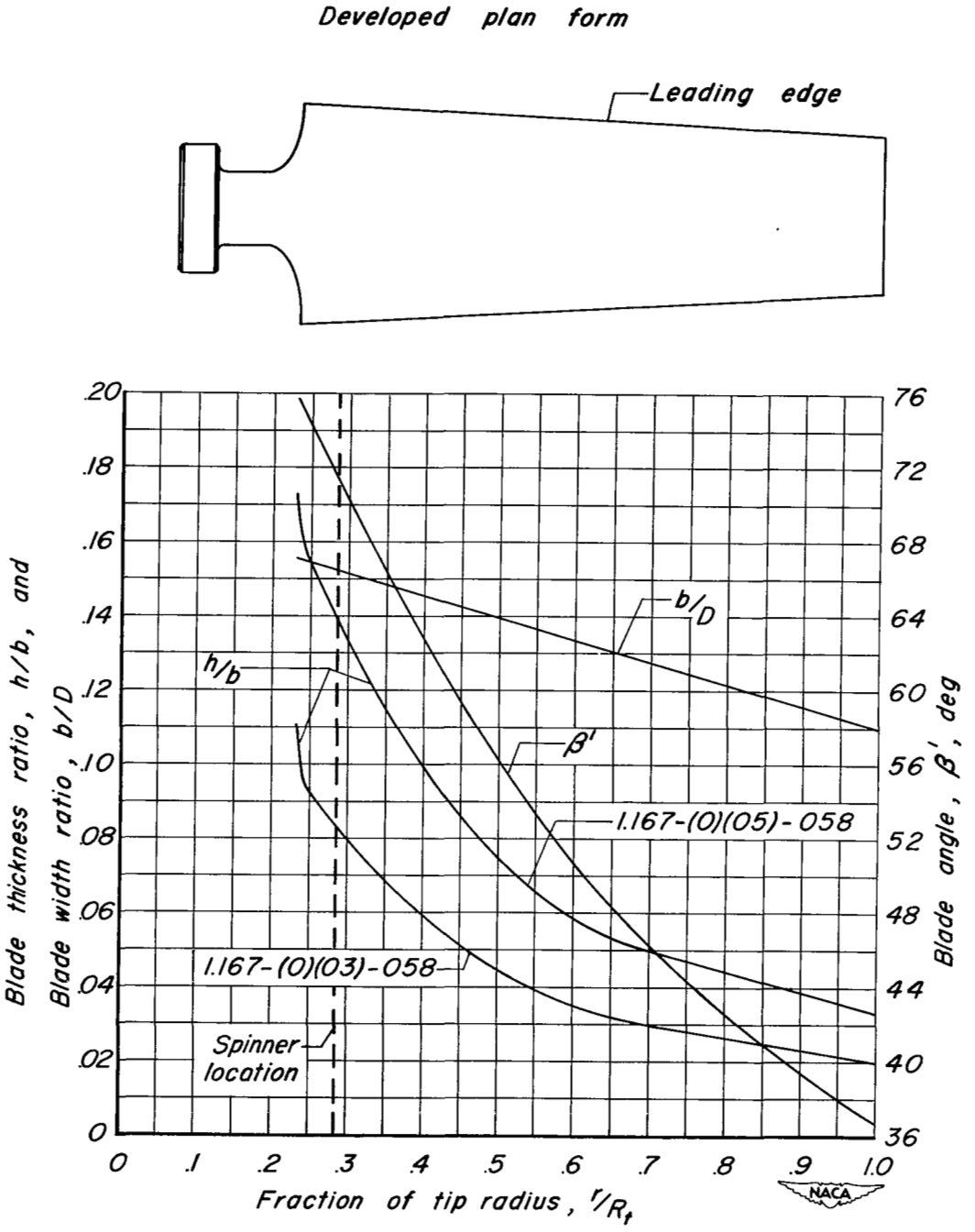

Figure 4.- Blade-form curves for the NACA 1.167-(0)(03)-058 and the NACA 1.167-(0)(05)-058 three-blade propellers.

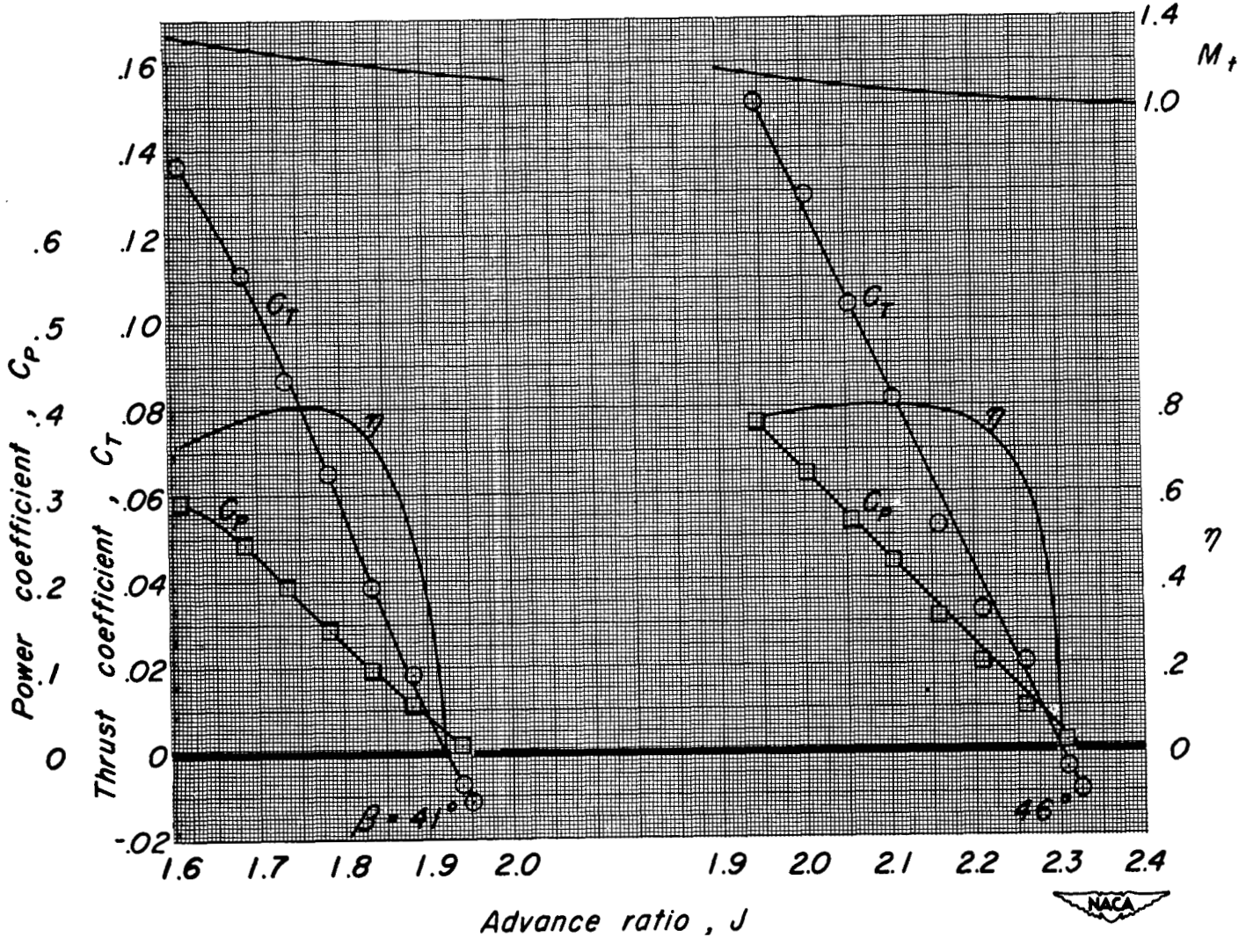

(a) M, 0.60; A, 0.27°

Figure 5.- Characteristics of the NACA 1.167-(0)(03)-058 propeller; R, 1,600,000; α, 0°.

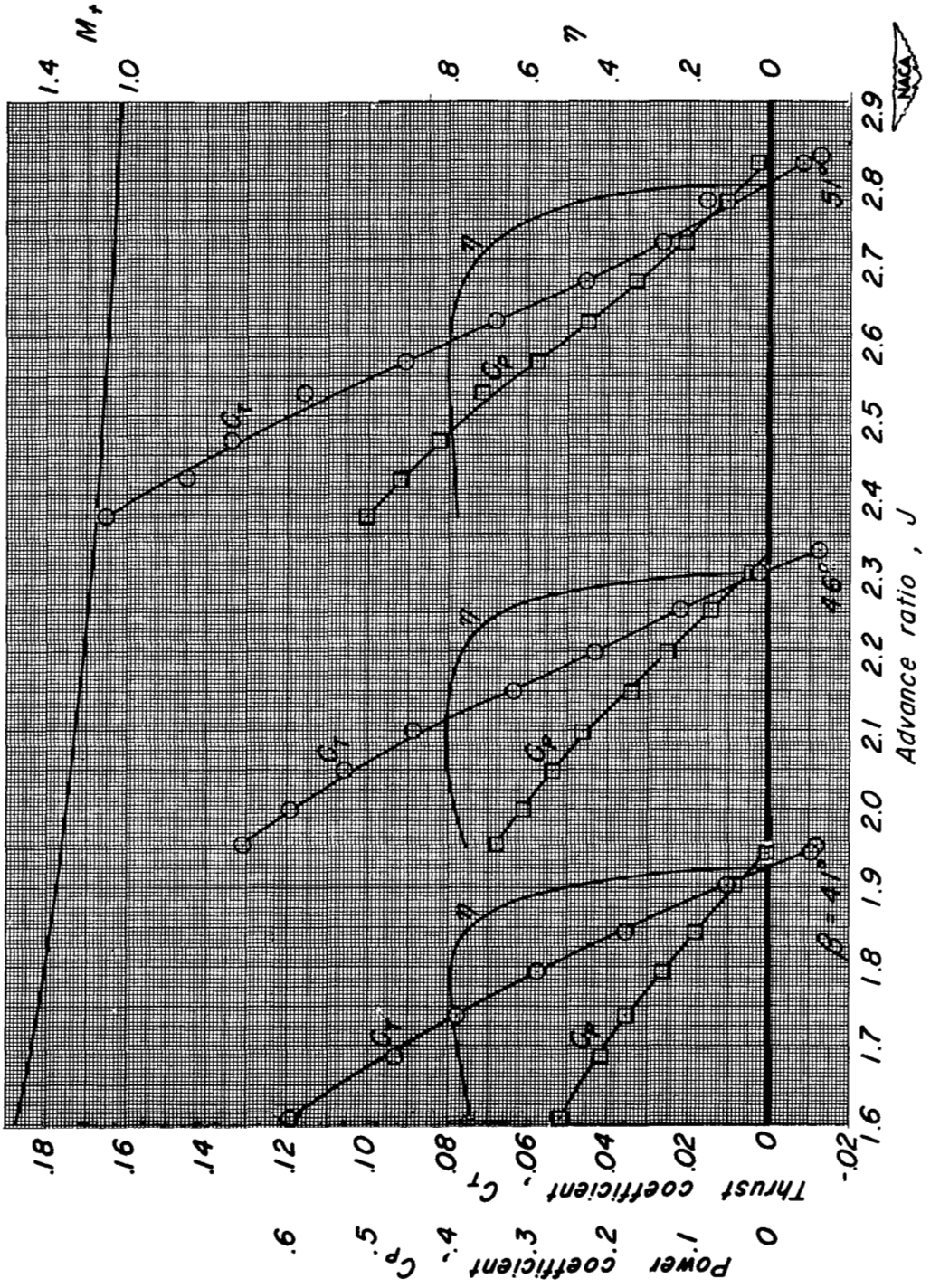

(b) M, 0.70; A, 0.27°

Figure 5.- Continued.

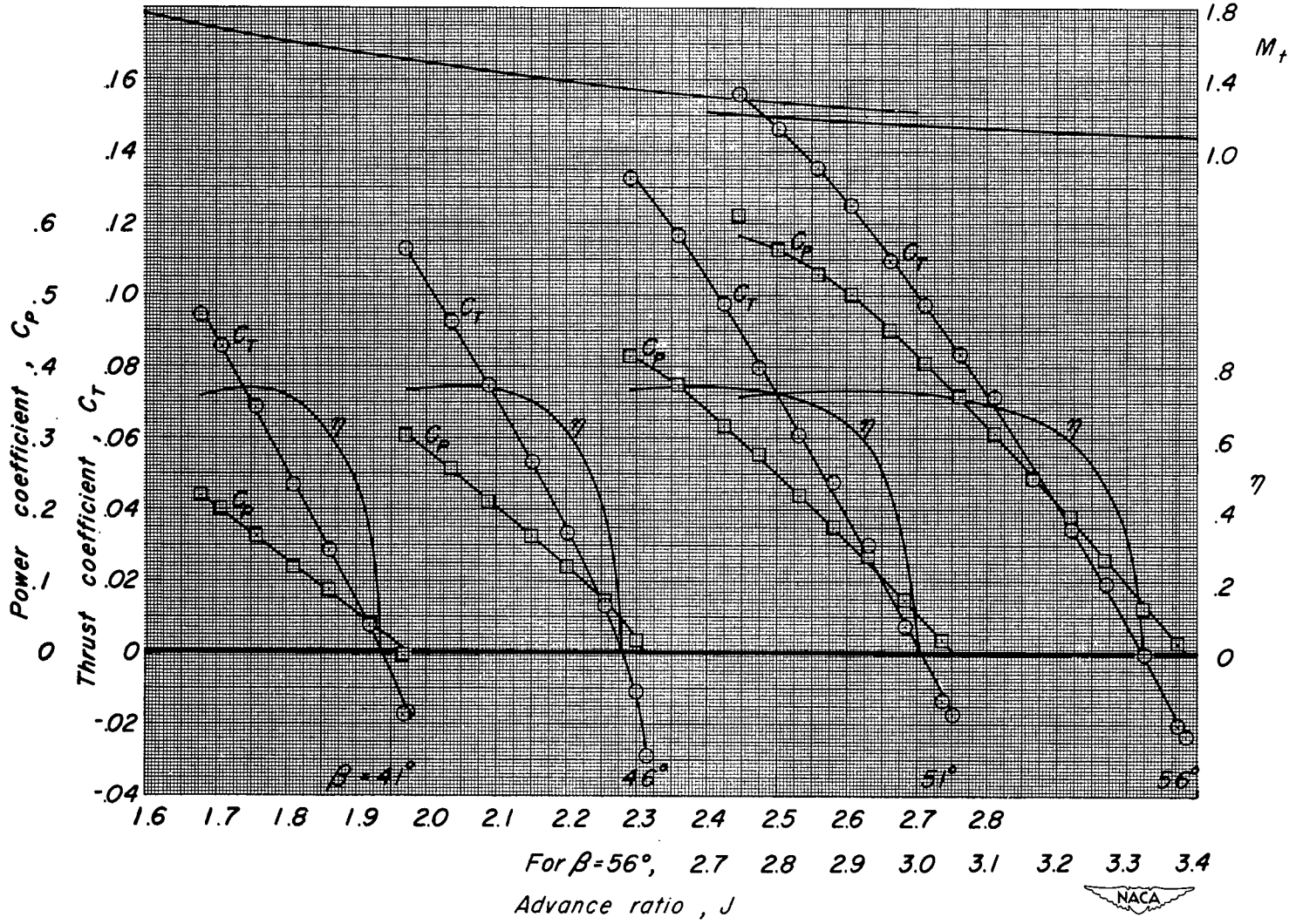

(c) M, 0.80; A, 0.25°

Figure 5.- Continued.

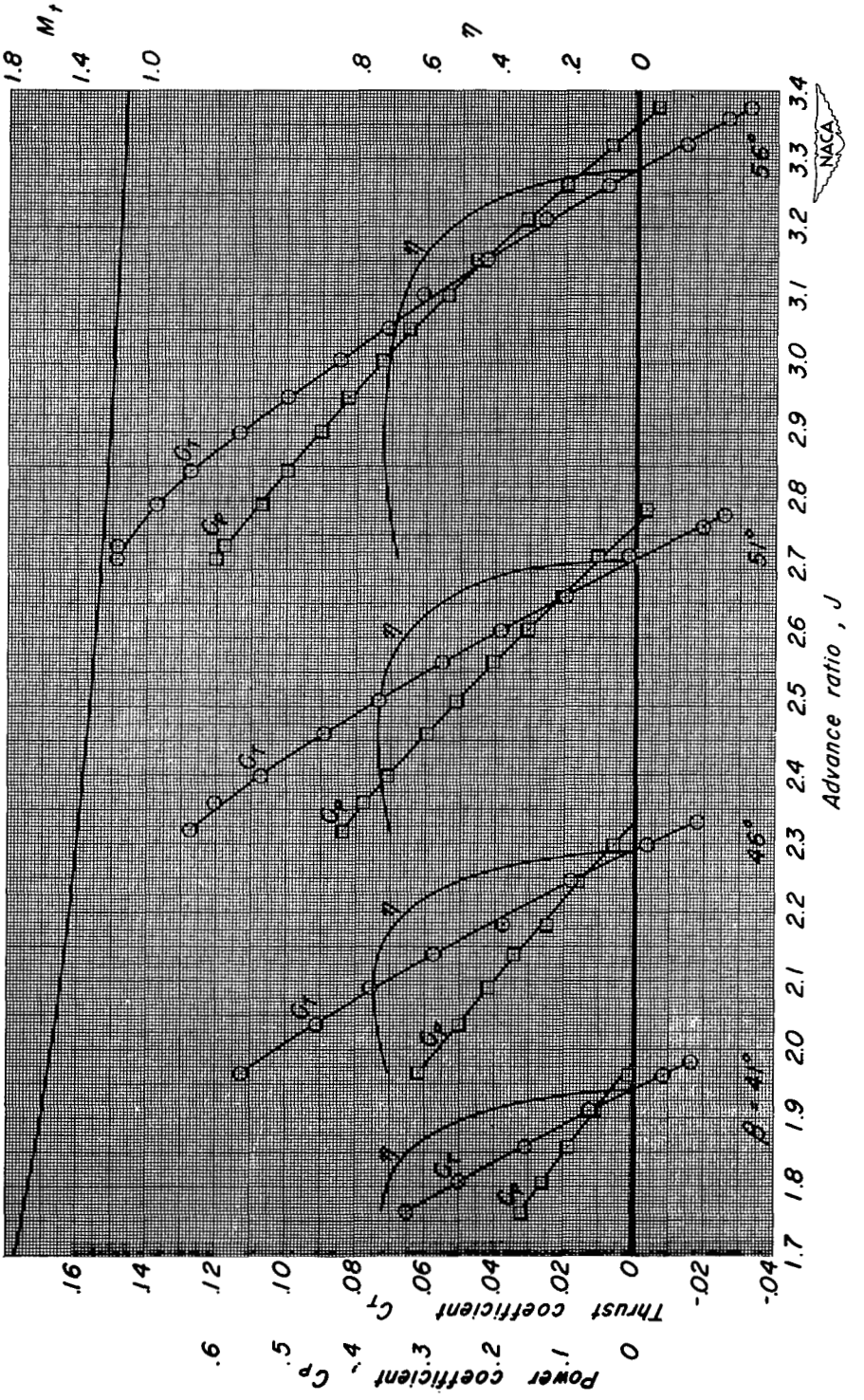

(d) M, 0.83: A, 0.23°

Figure 5.- Continued.

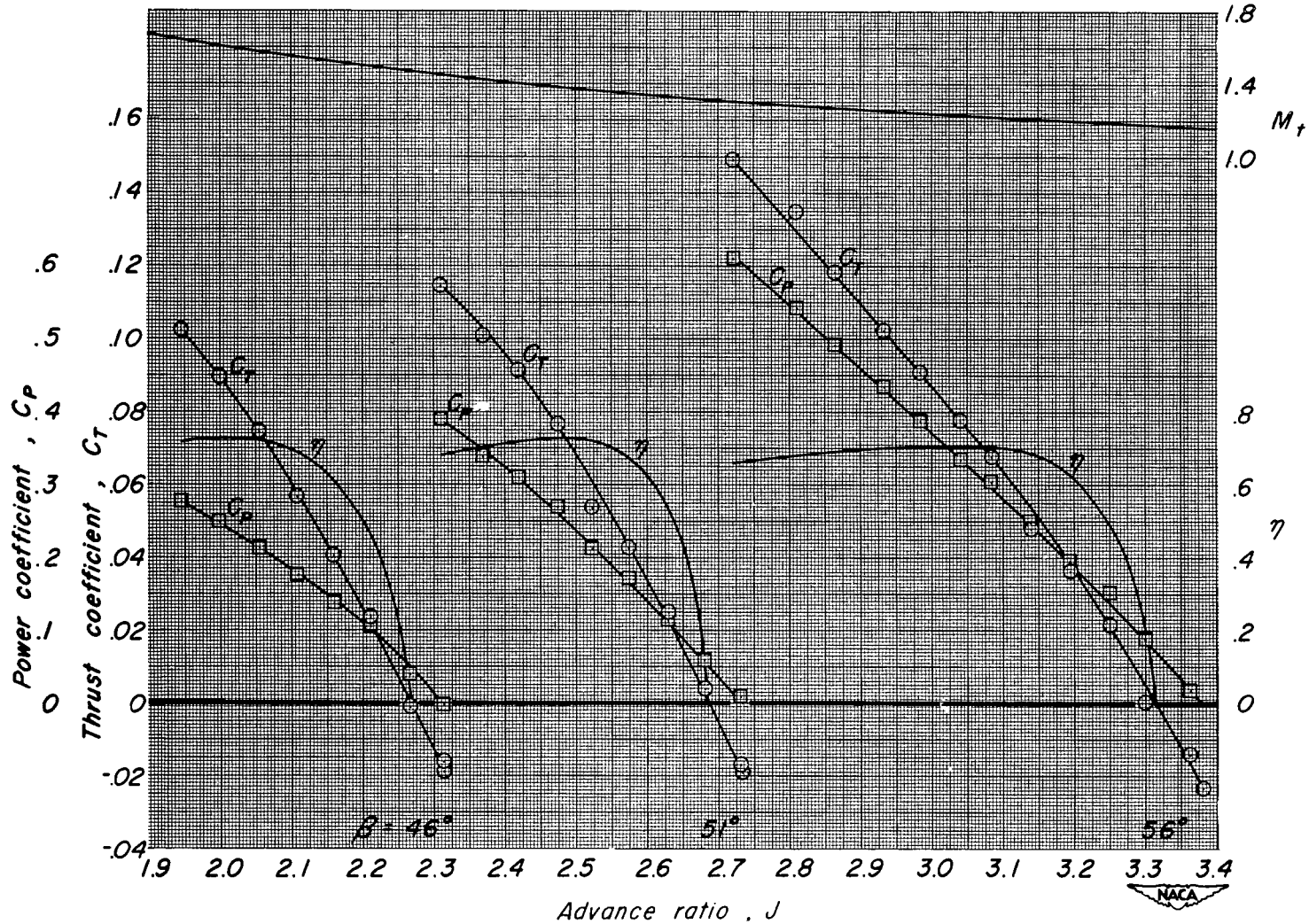

(e) M, 0.86; A, 0.22°

Figure 5.- Continued.

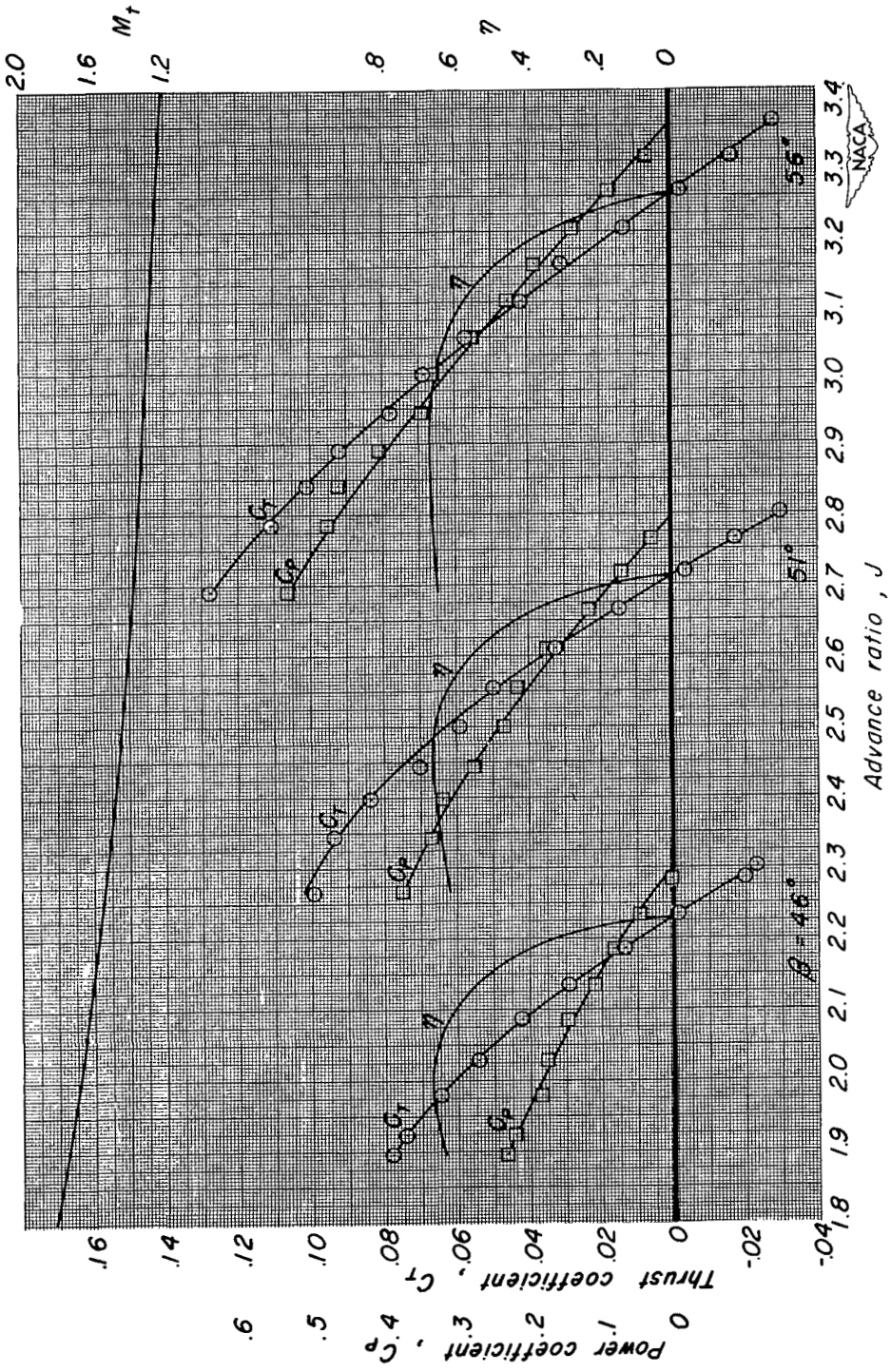

(f) M, 0.90; A, 0.18°

Figure 5.- Continued.

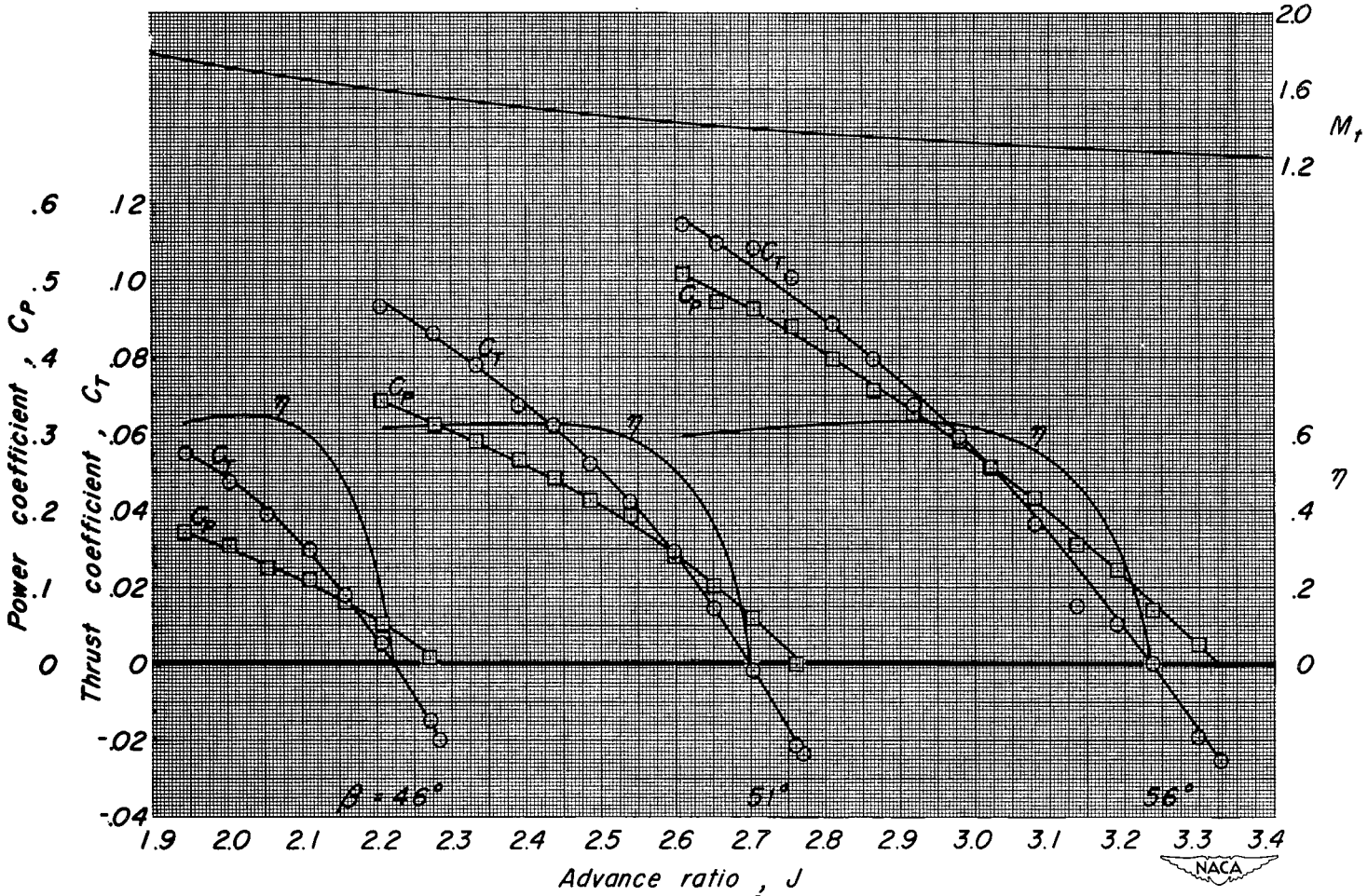

(g) M, 0.92; A, 0.18°

Figure 5.- Concluded.

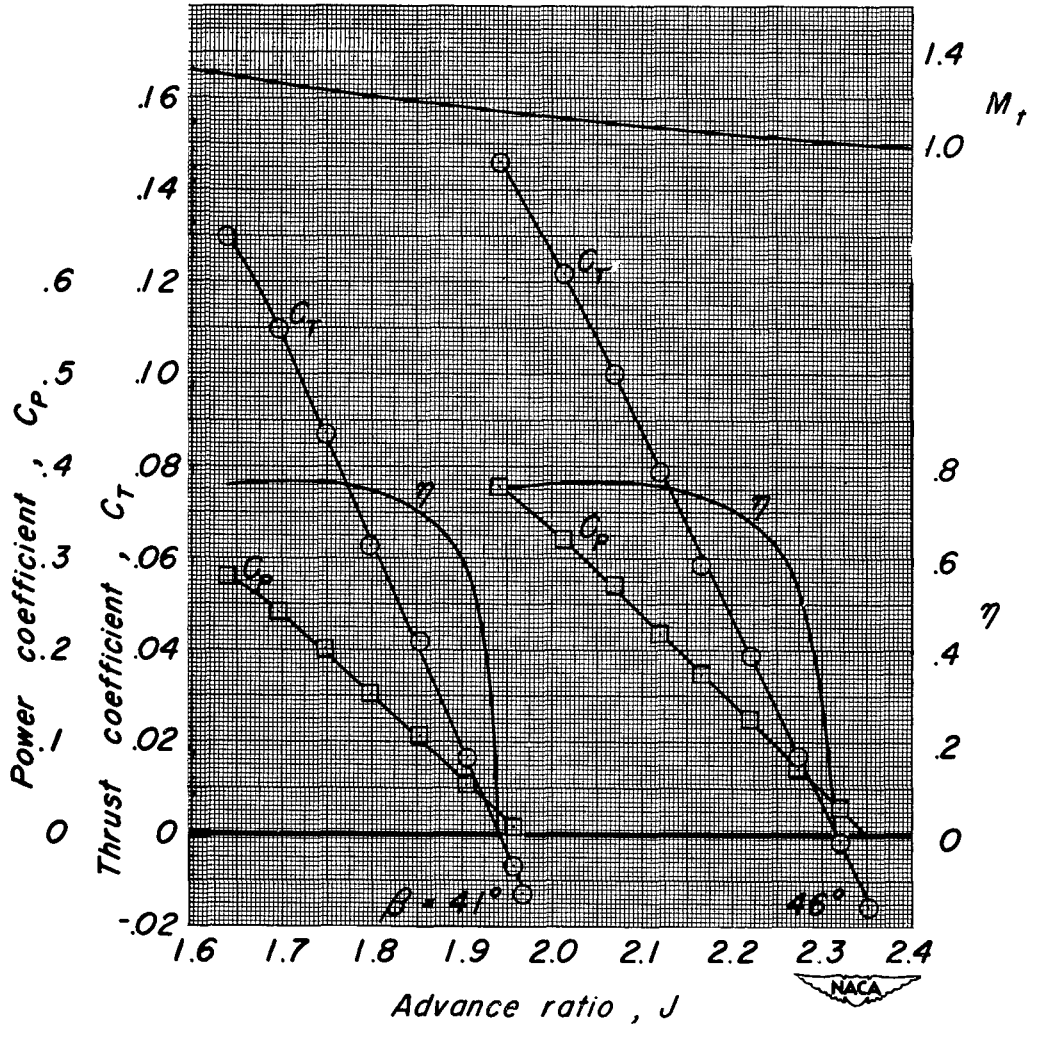

(a) M, 0.60; A, 4.95°

Figure 6.- Characteristics of the NACA 1.167-(0)(03)-058 propeller; R, 1,600,000; α, 3.92°.

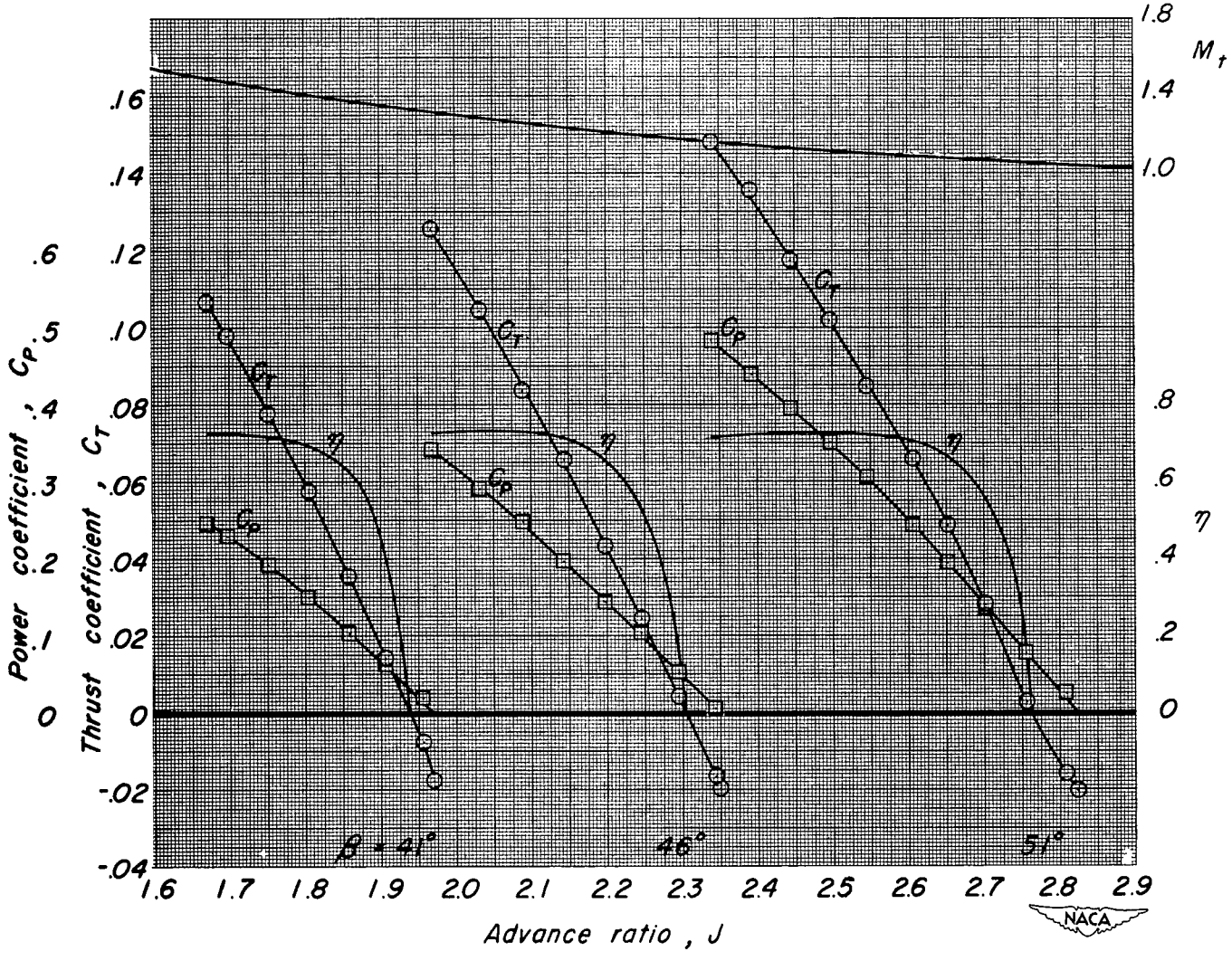

(b) M, 0.70; A, 4.92°

Figure 6.- Continued.

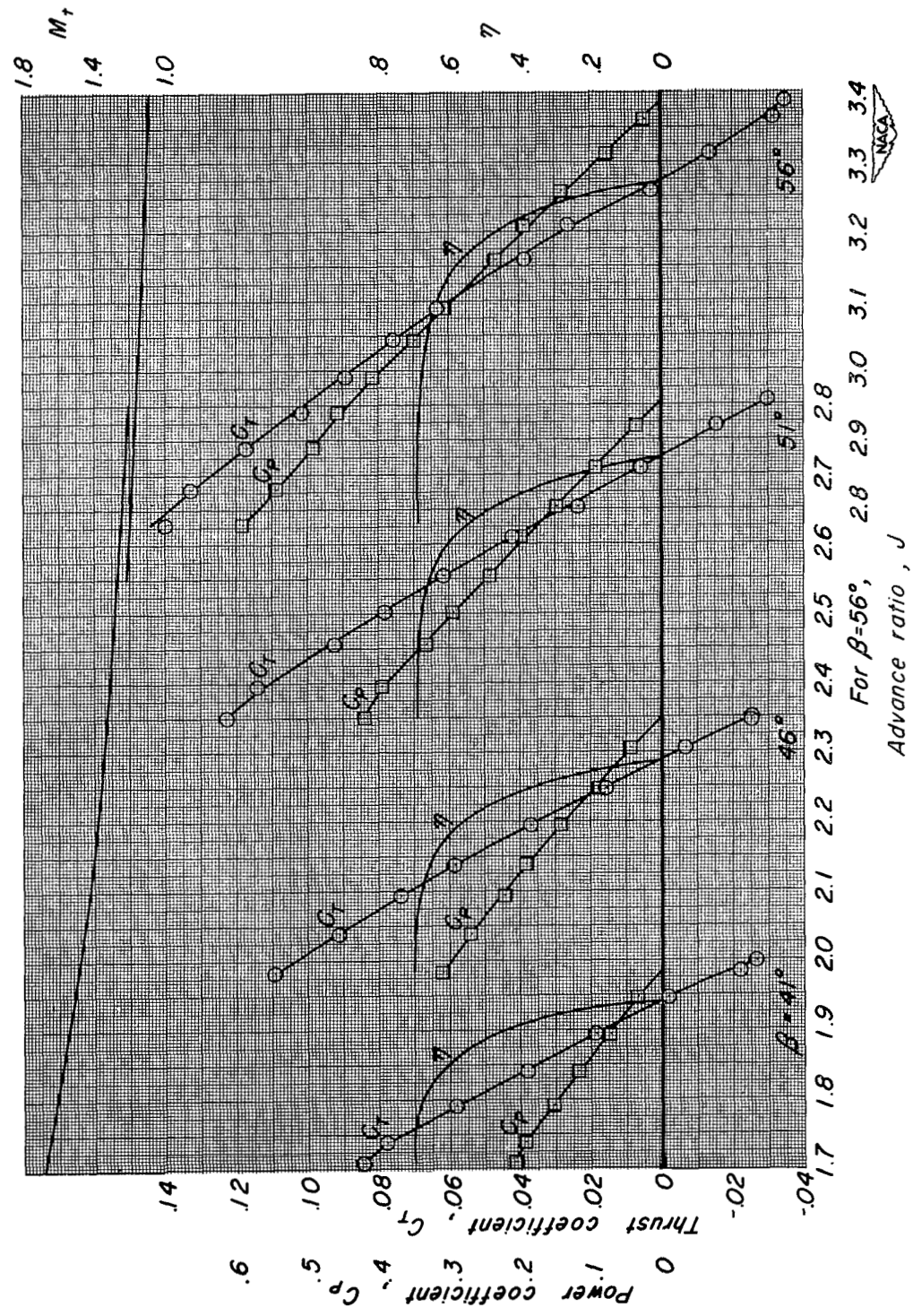

(c) M, 0.80; A, 4.75°

Figure 6.- Continued.

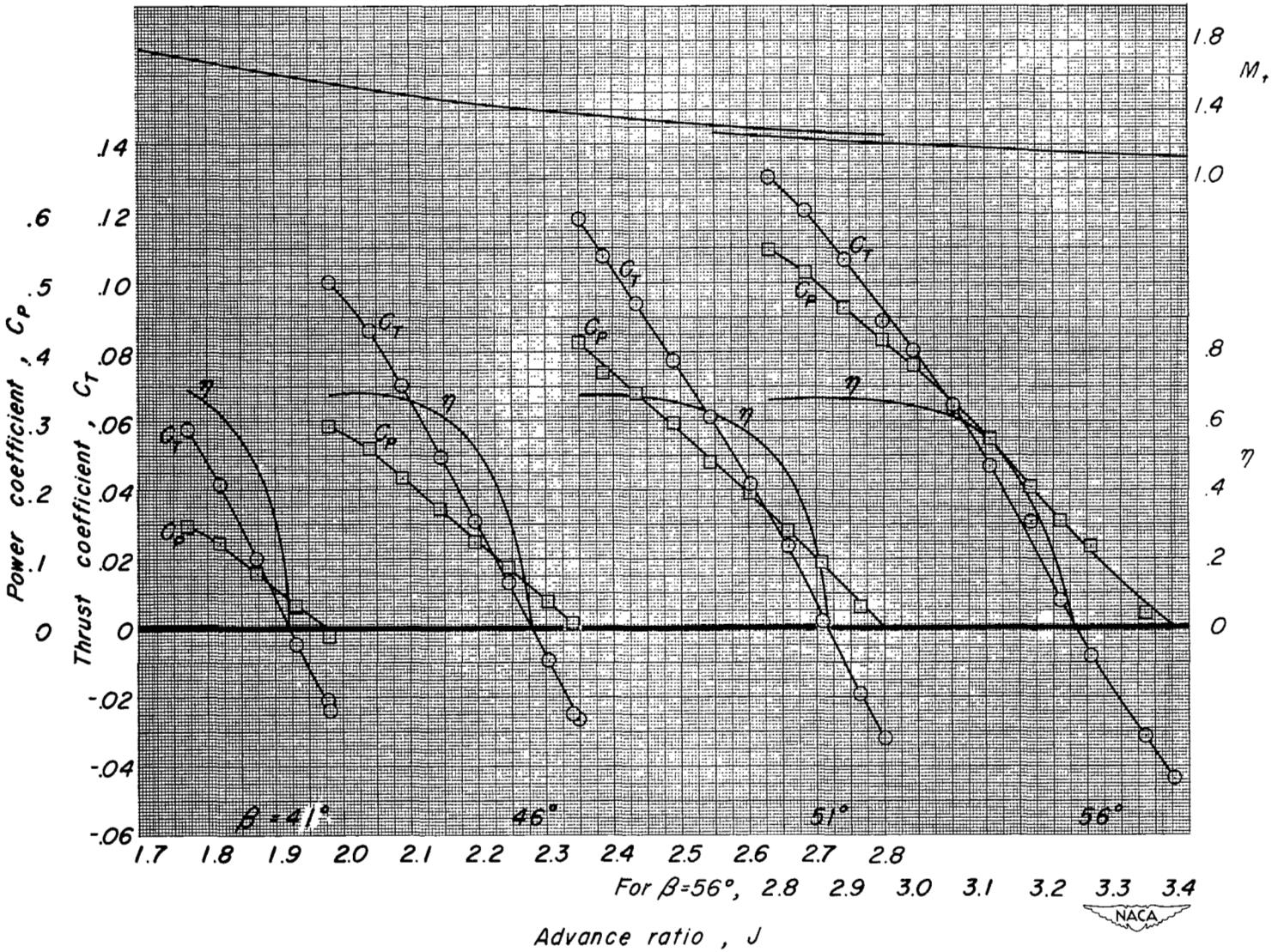

(d) M, 0.83; A, 4.68°

Figure 6.- Continued.

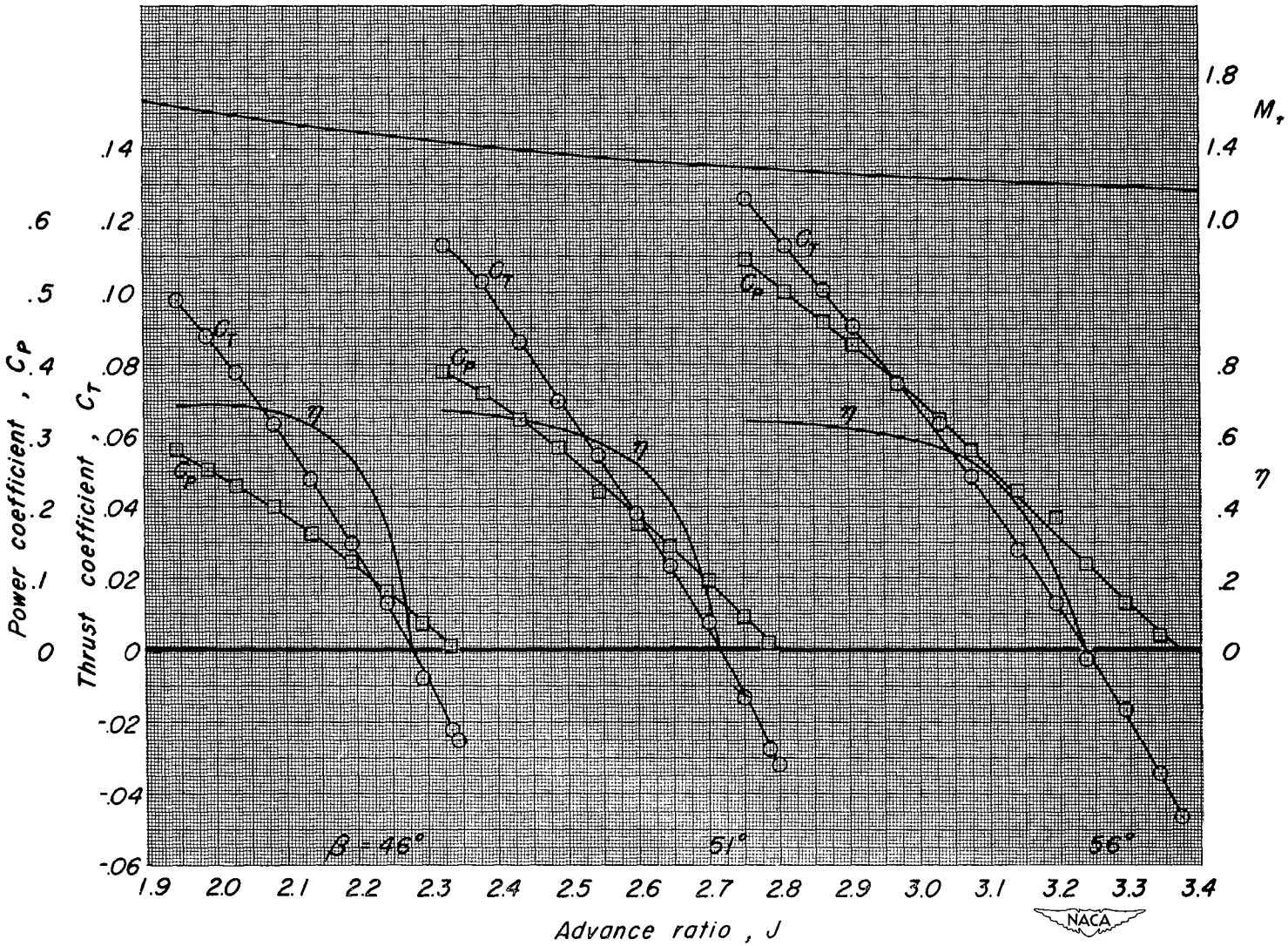

(e) M, 0.86; A, 4.60°

Figure 6.- Continued.

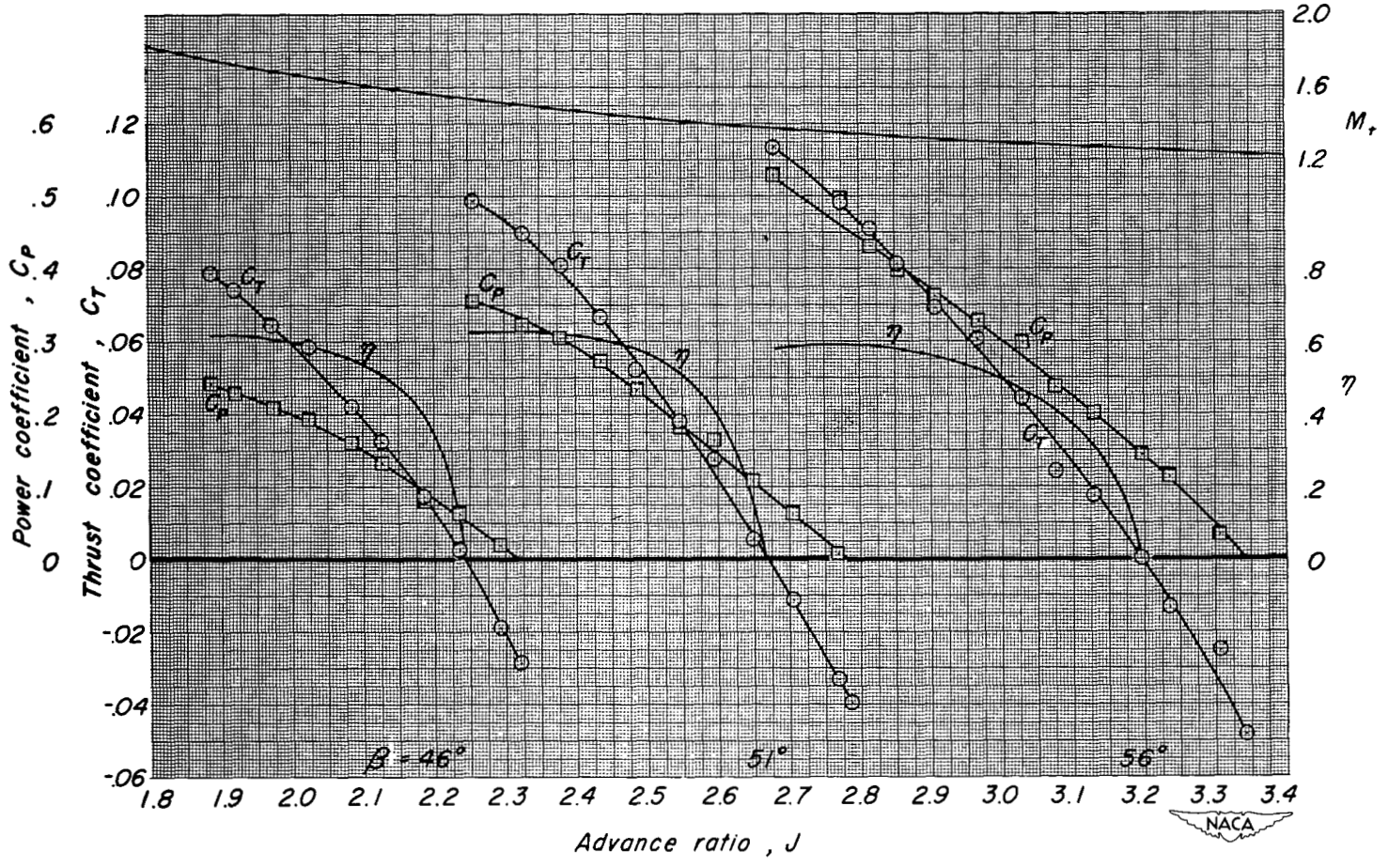

(f) M, 0.90; A, 4.52°

Figure 6.- Continued.

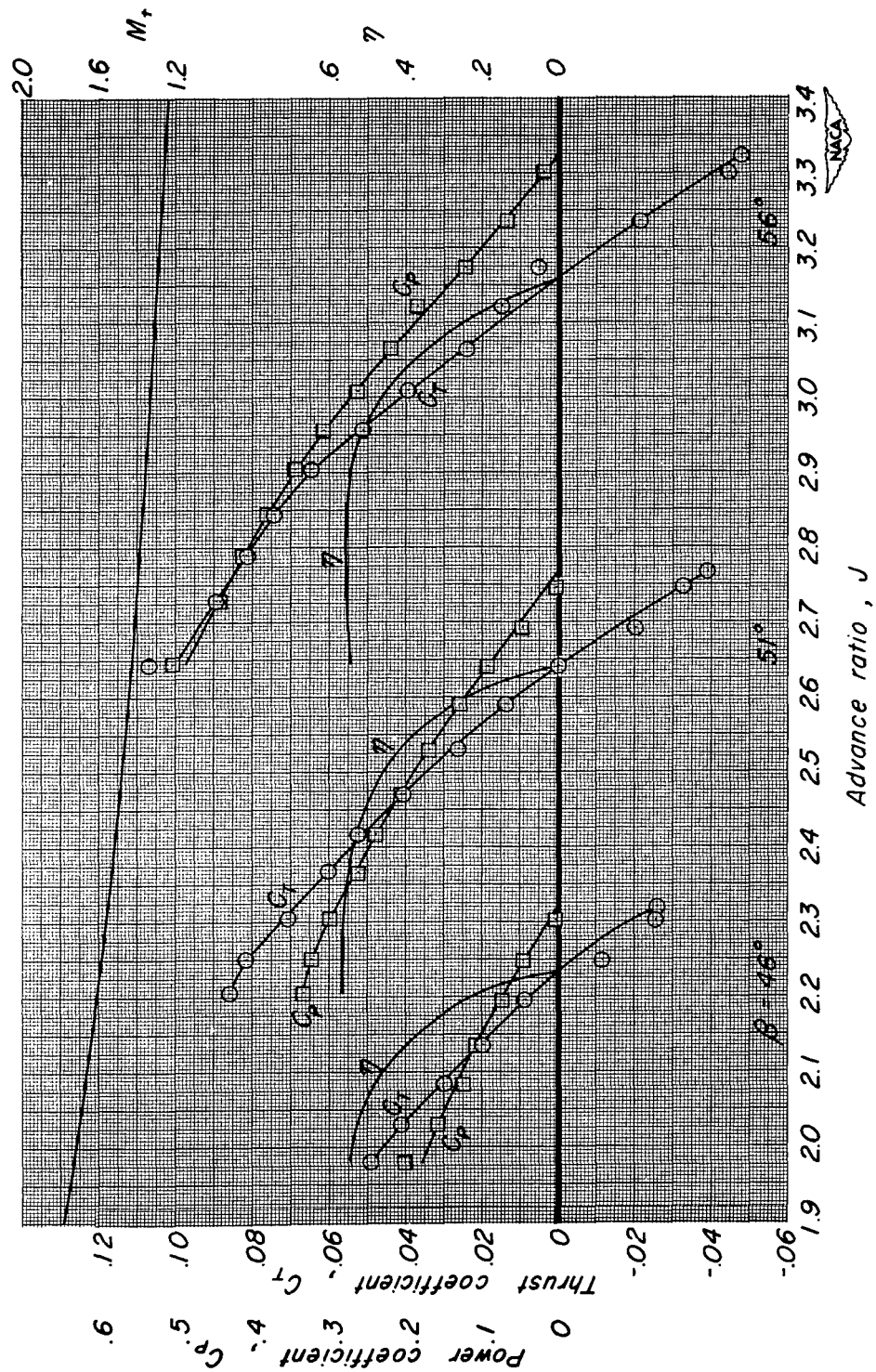

(g) M, 0.92; A, 4.48°

Figure 6.- Concluded.

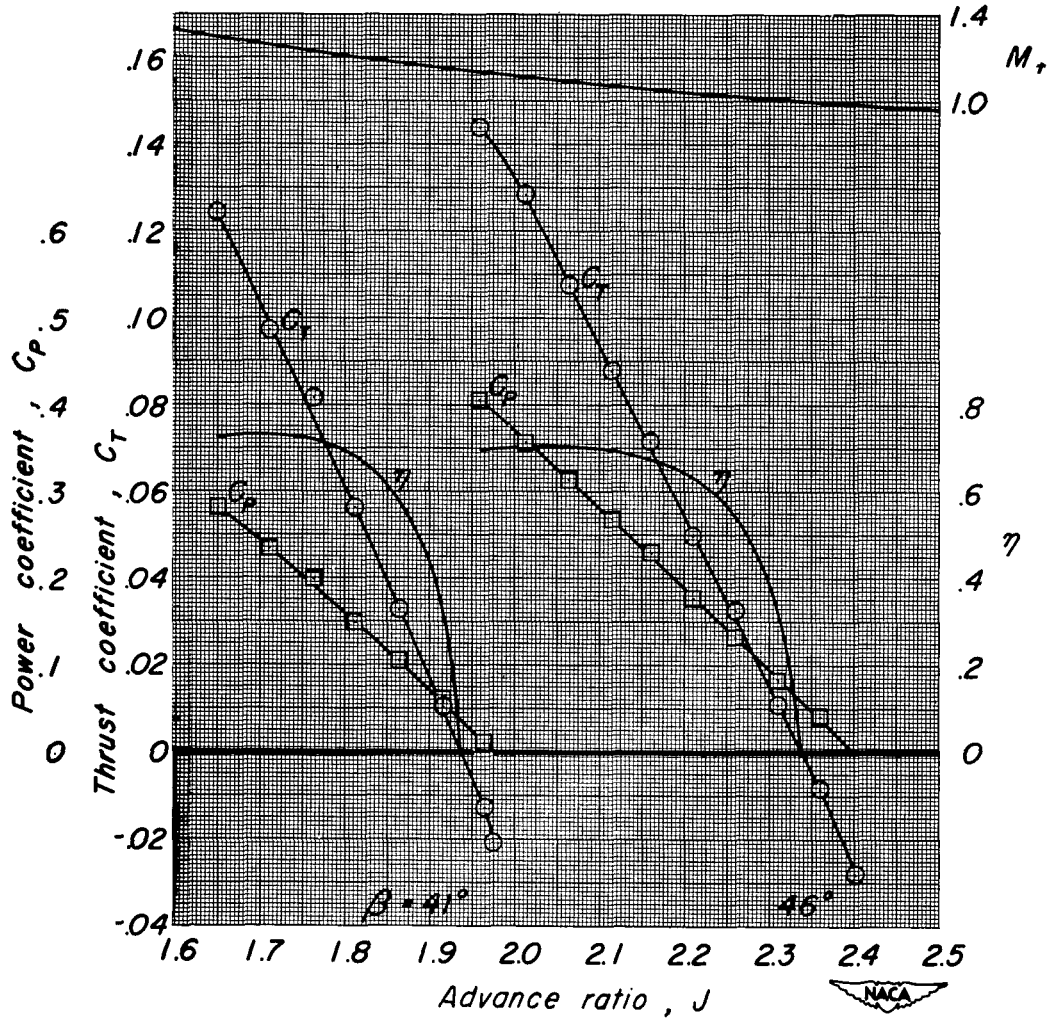

(a) M, 0.60; A, 7.20°

Figure 7.- Characteristics of the NACA 1.167-(0)(03)-058 propeller; R, 1,600,300; α, 5.88°.

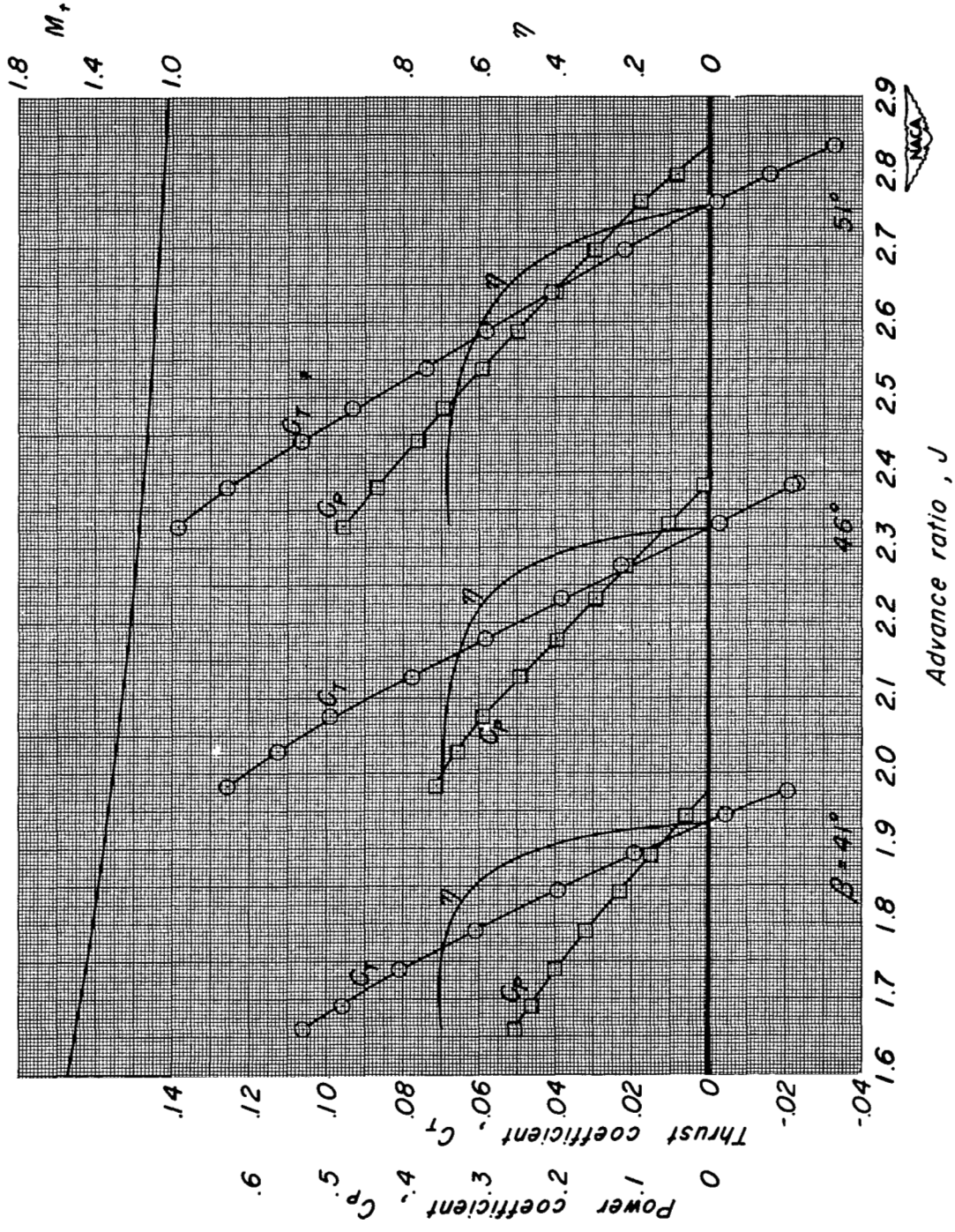

(b) M, 0.70; A, 7.12°

Figure 7.- Continued.

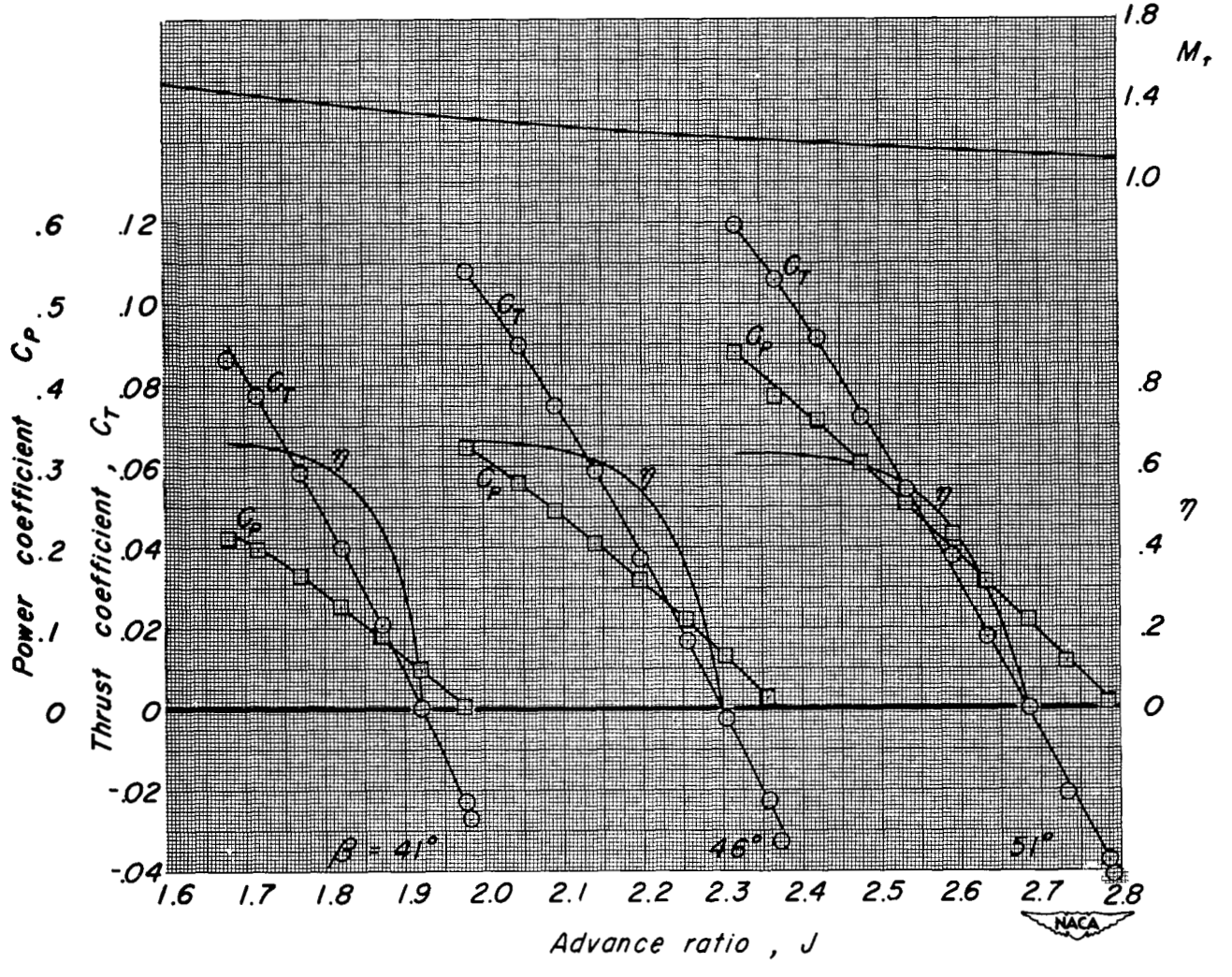

(c) M, 0.80; A, 6.95°

Figure 7.- Concluded.

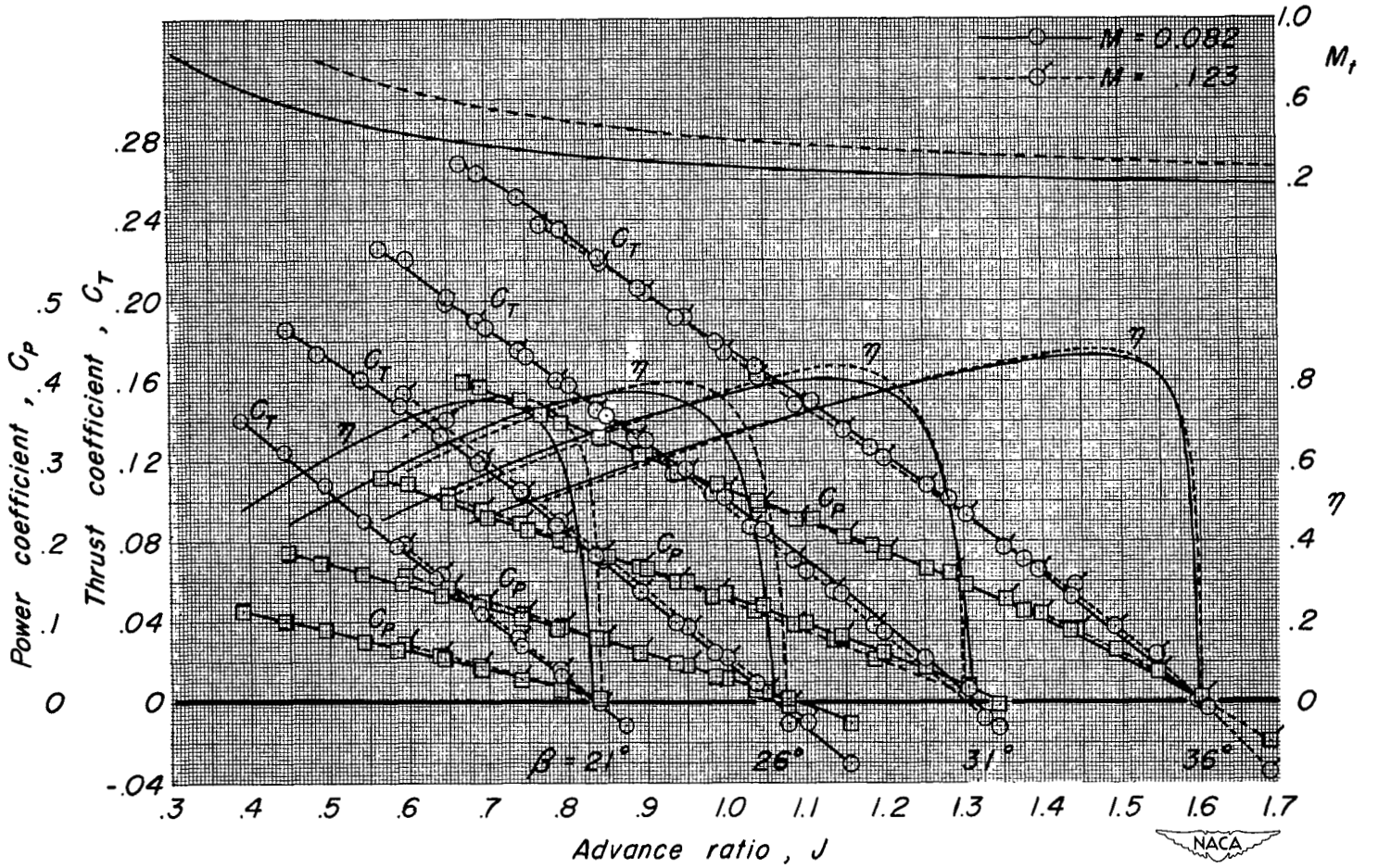

(a) α, 0°; A, 0.20°

Figure 8.- Characteristics of the NACA 1.167-(0)(05)-058 propeller; R, 3,200,000.

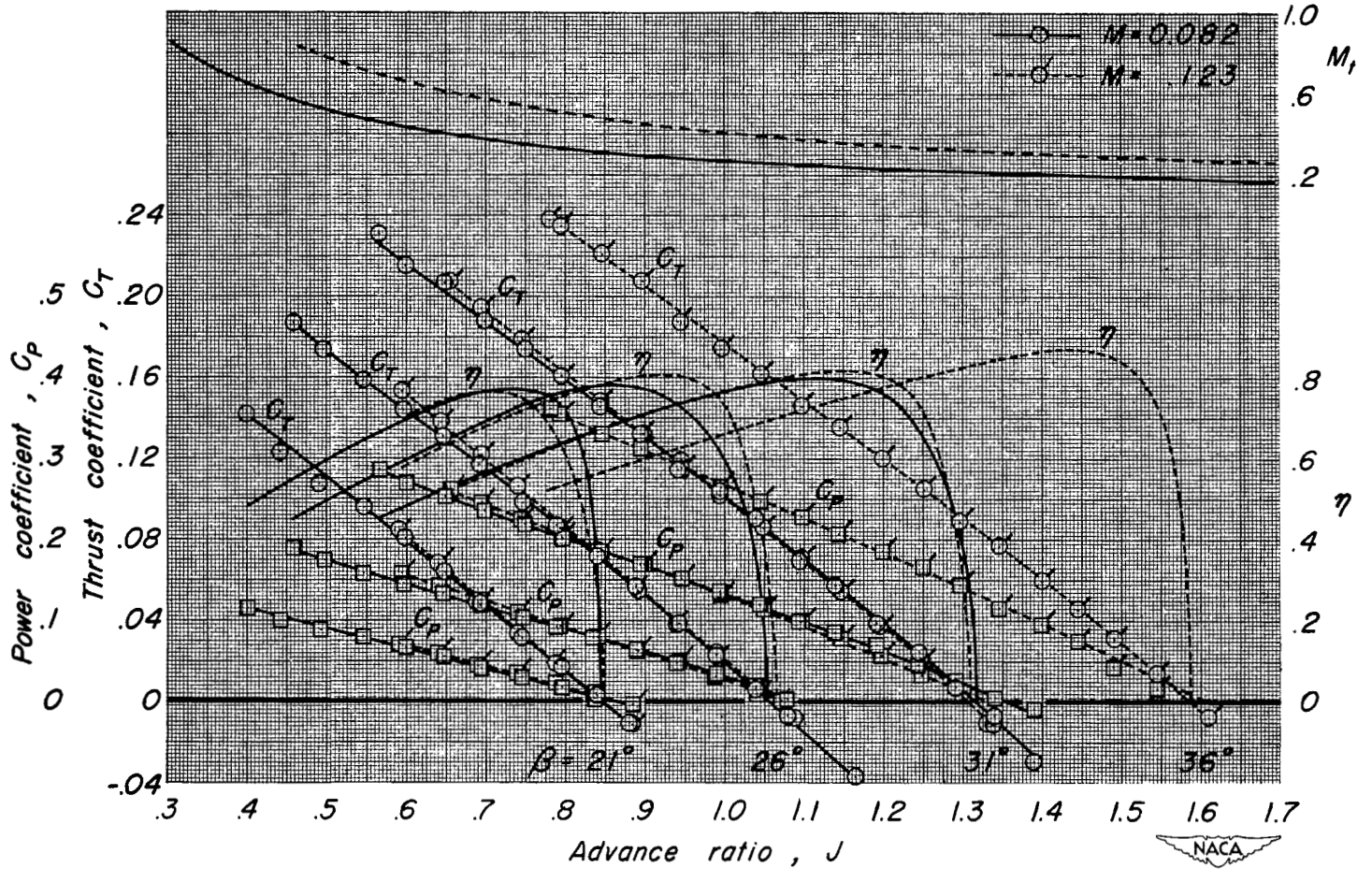

(b) α, 3.92°; A, 4.72°

Figure 8.- Continued.

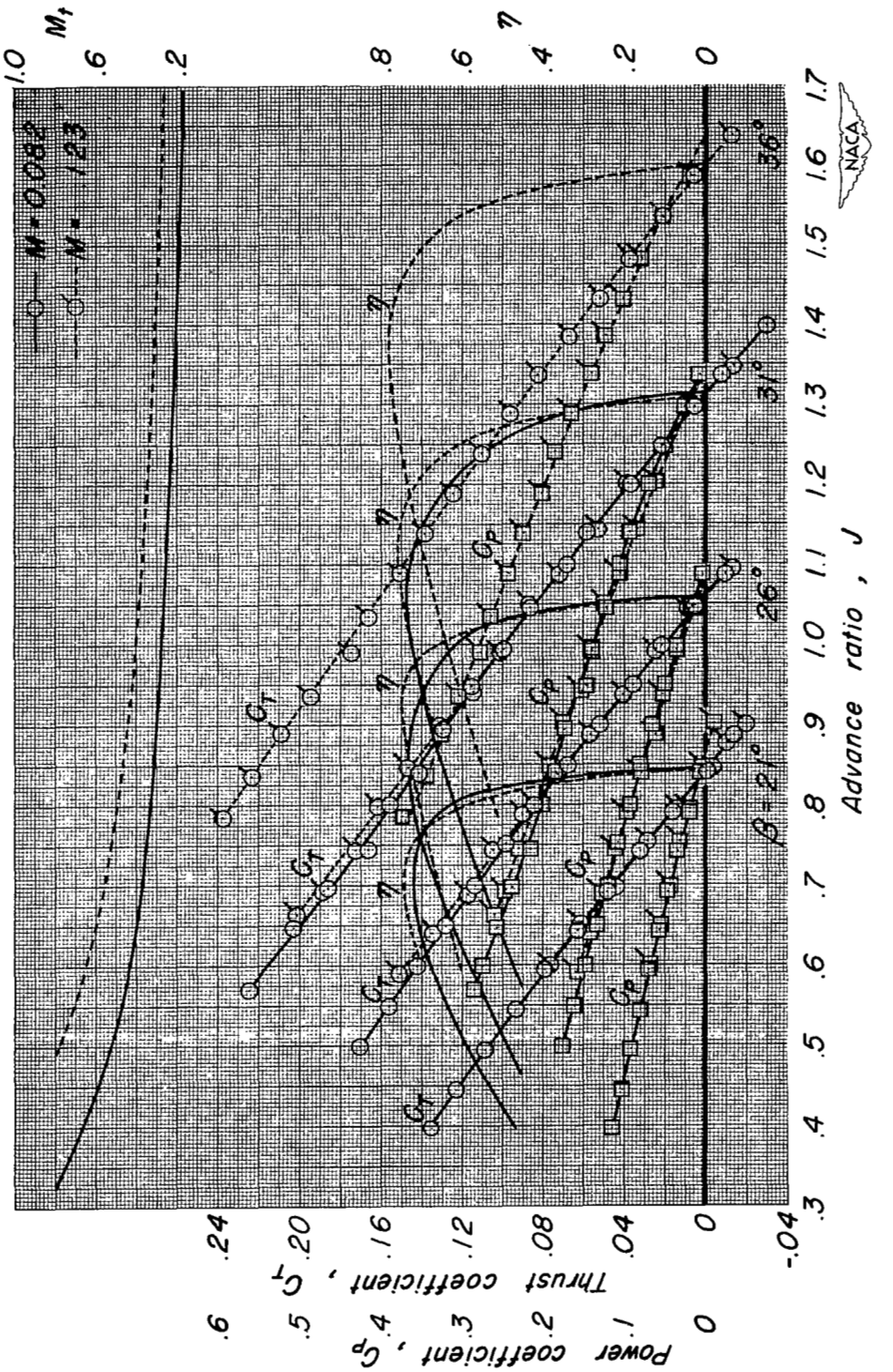

(c) α, 7.84°; A, 9.68°

Figure 8.- Continued.

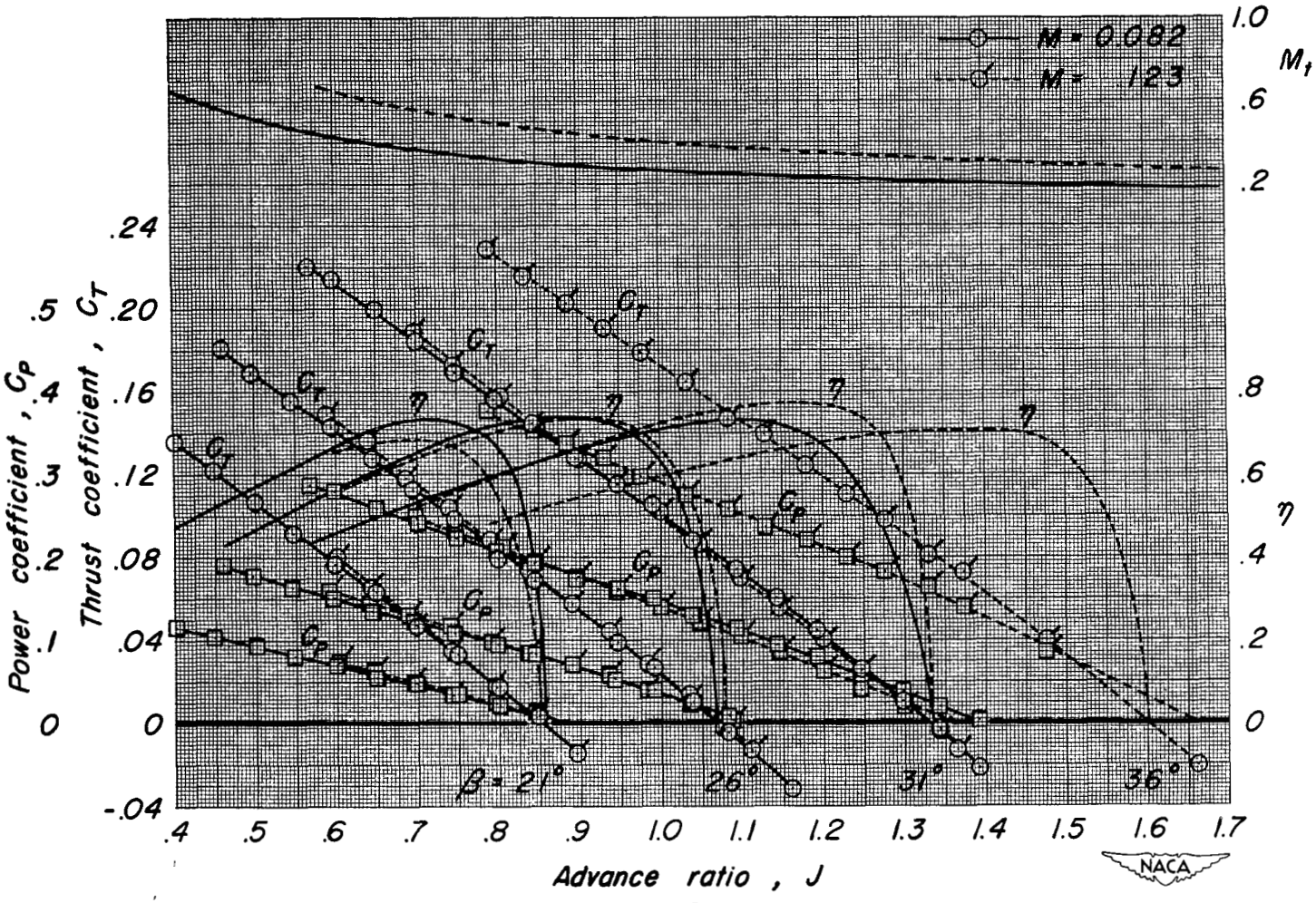

(d) α, 11.76°; A, 14.05°

Figure 8.- Continued.

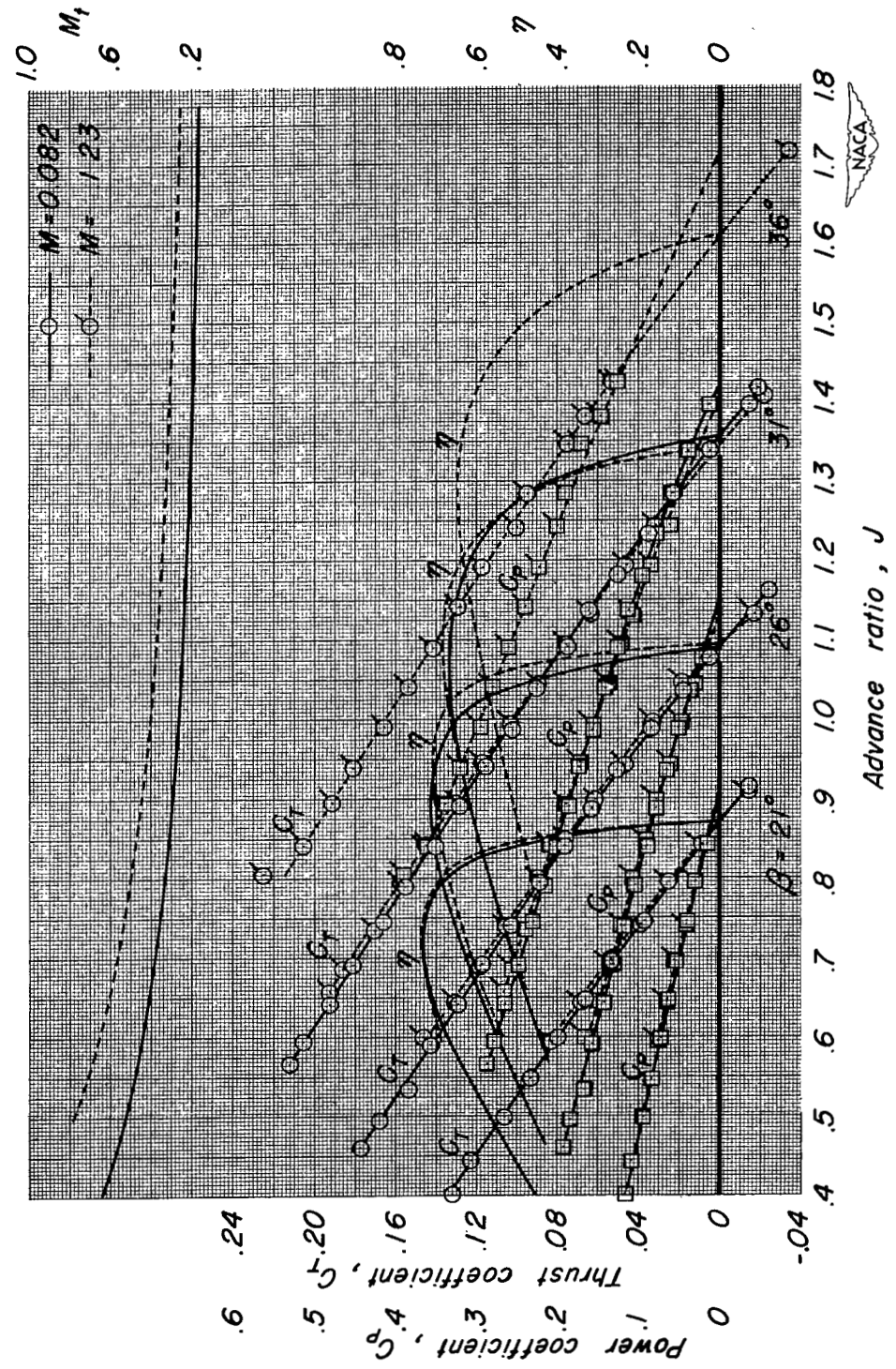

(e) α, 15.68°; A, 18.77°

Figure 8.- Concluded.

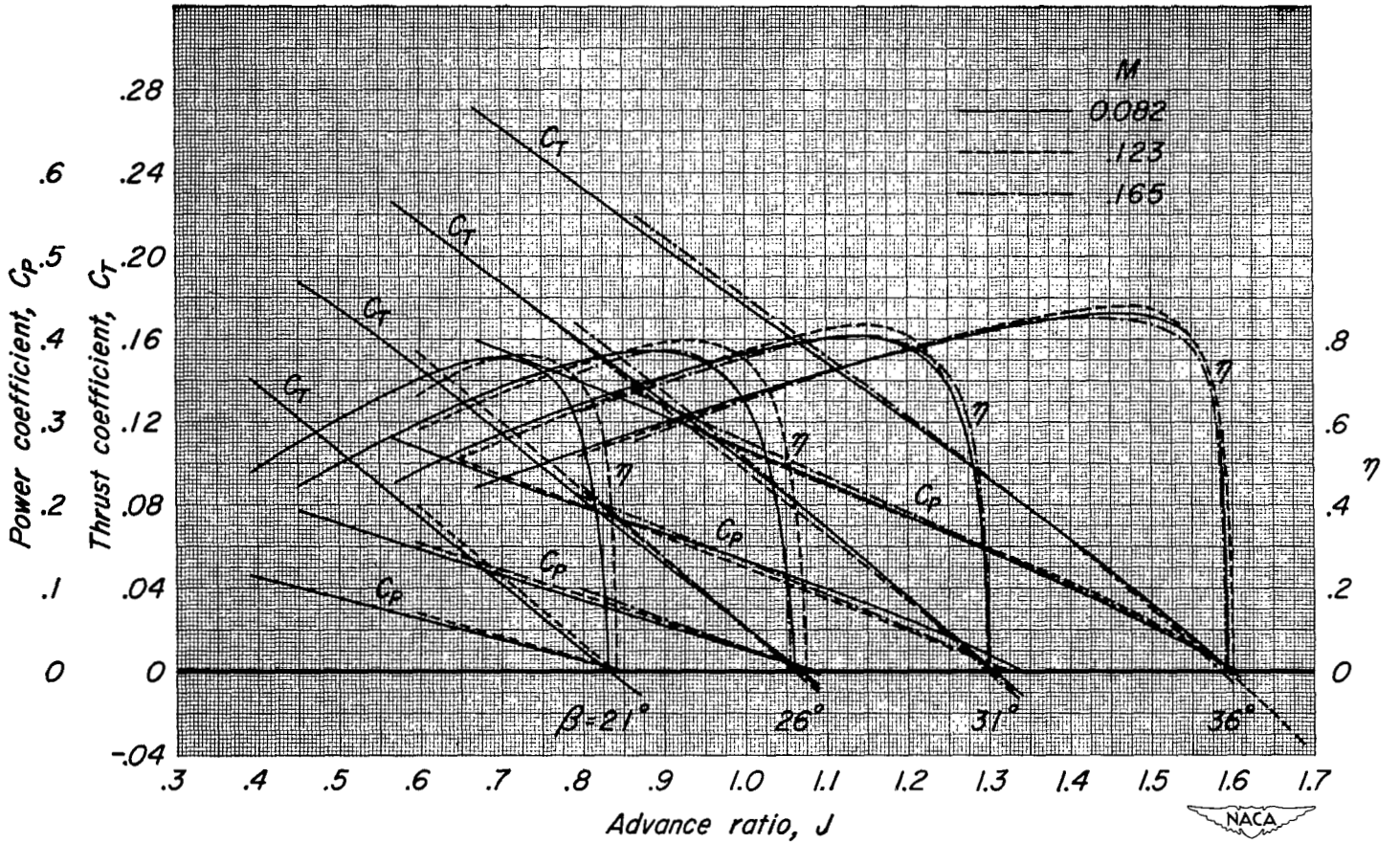

Figure 9.- The effect of Mach number on the characteristics of the NACA 1.167-(0)(05)-058 propeller; R, 3,200,000; α, 0°.

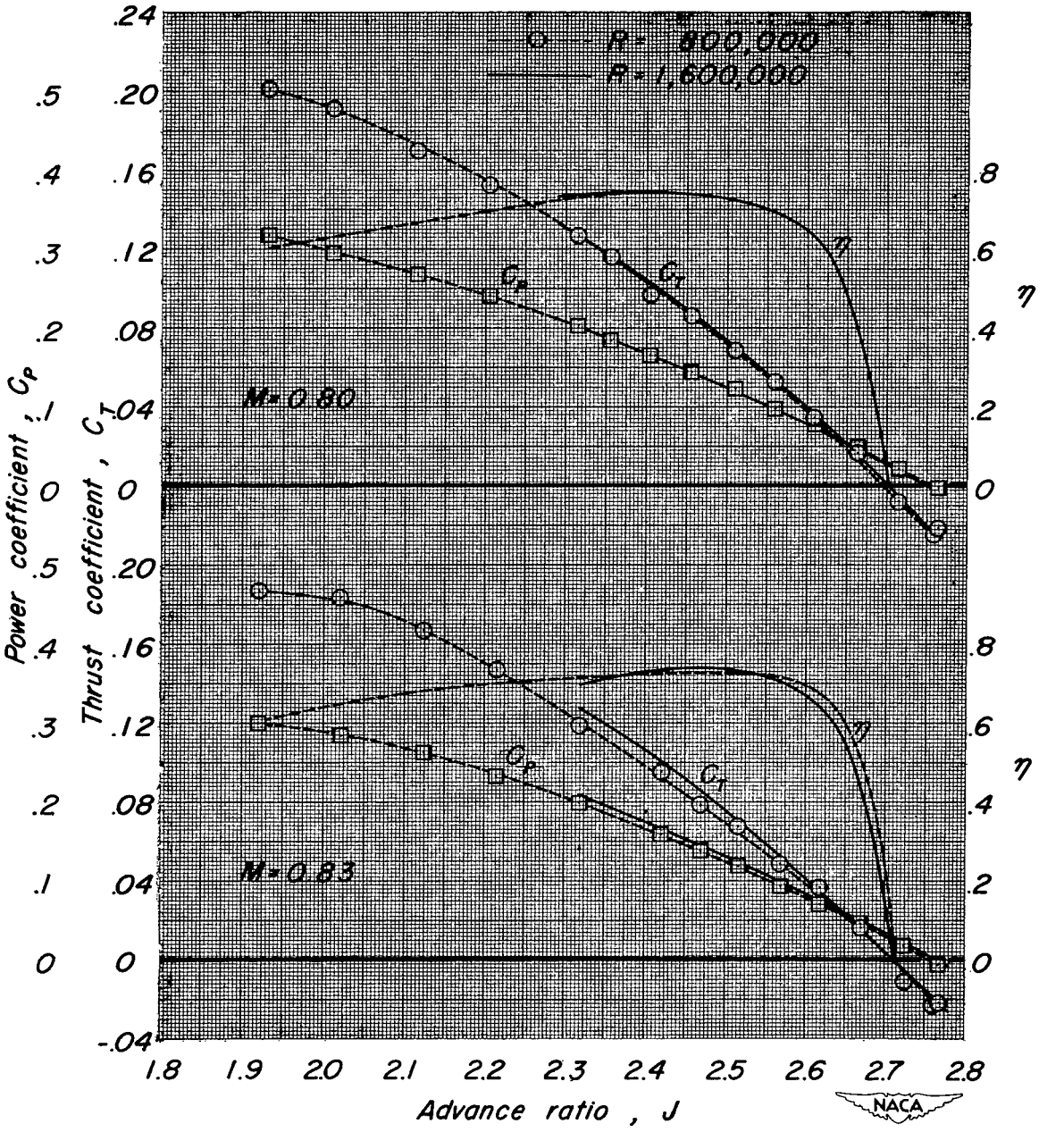

(a) M, 0.80 and 0.83

Figure 10.- The effect of Reynolds number on the characteristics of the NACA 1.167-(0)(03)-058 propeller; β, 51°; α, 0°.

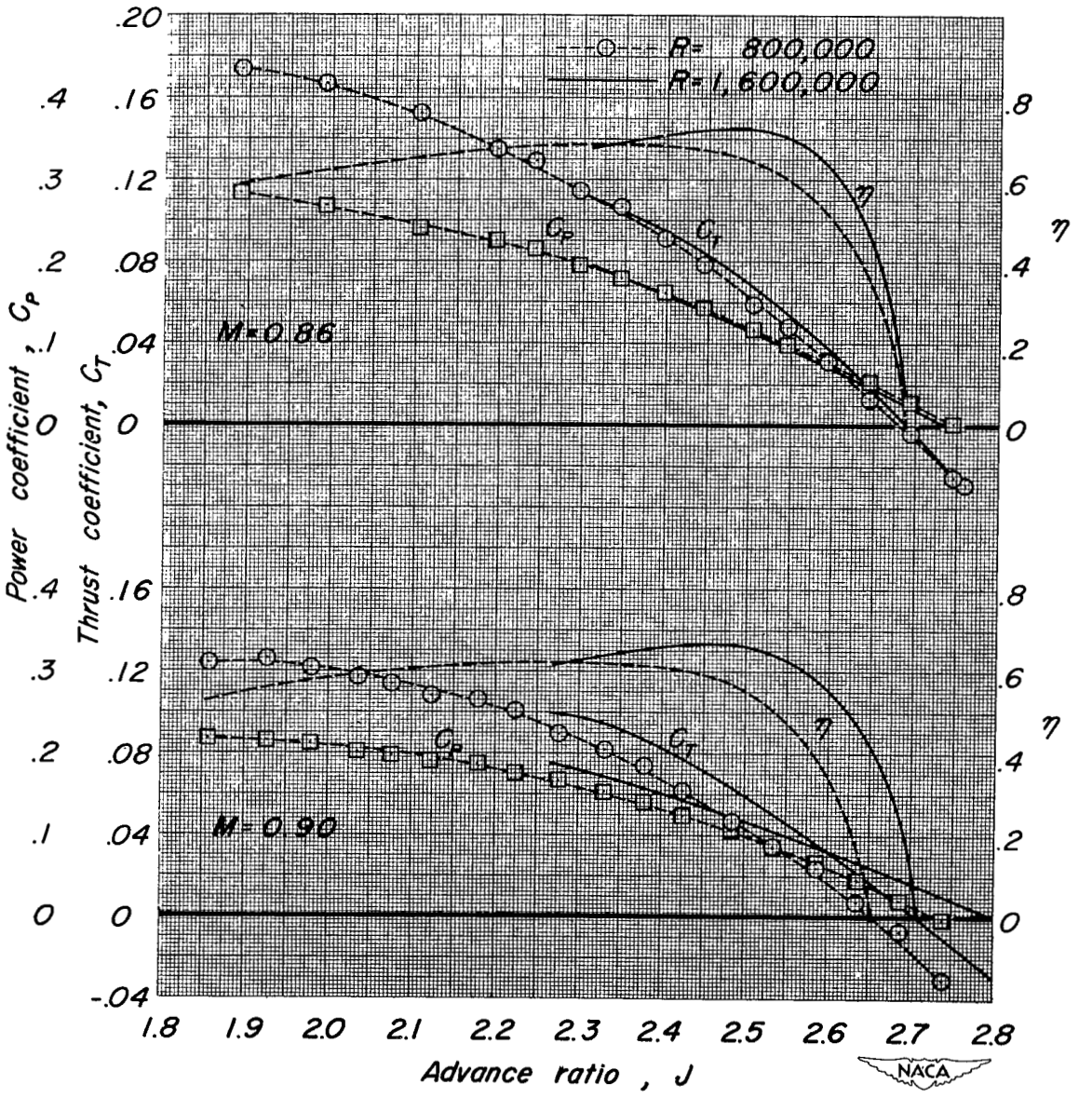

(b) M, 0.86 and 0.90

Figure 10.- Concluded.

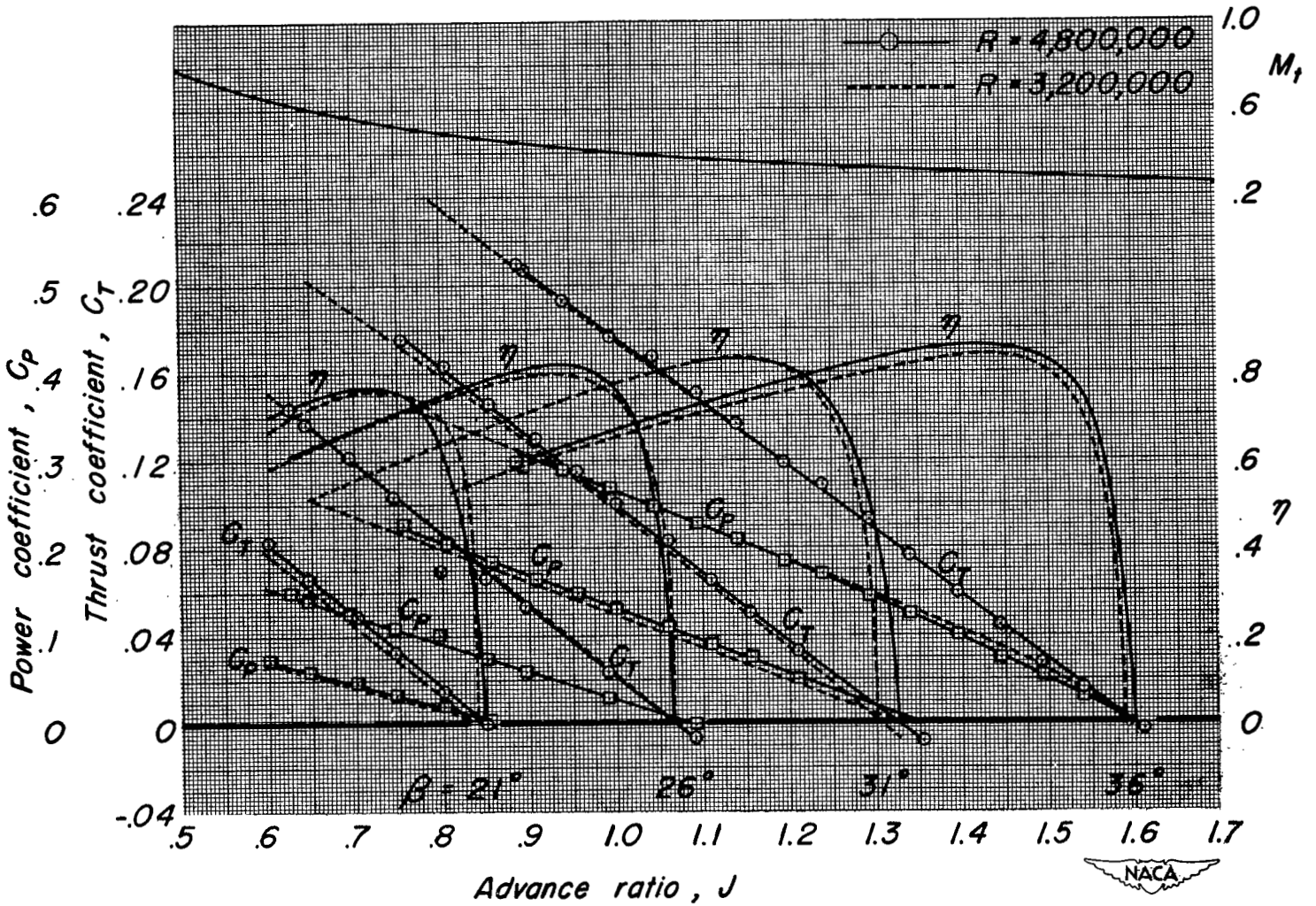

(a) M, 0.123

Figure 11.- The effect of Reynolds number on the characteristics of the NACA 1.167-(0)(05)-058 propeller; α, 0°.

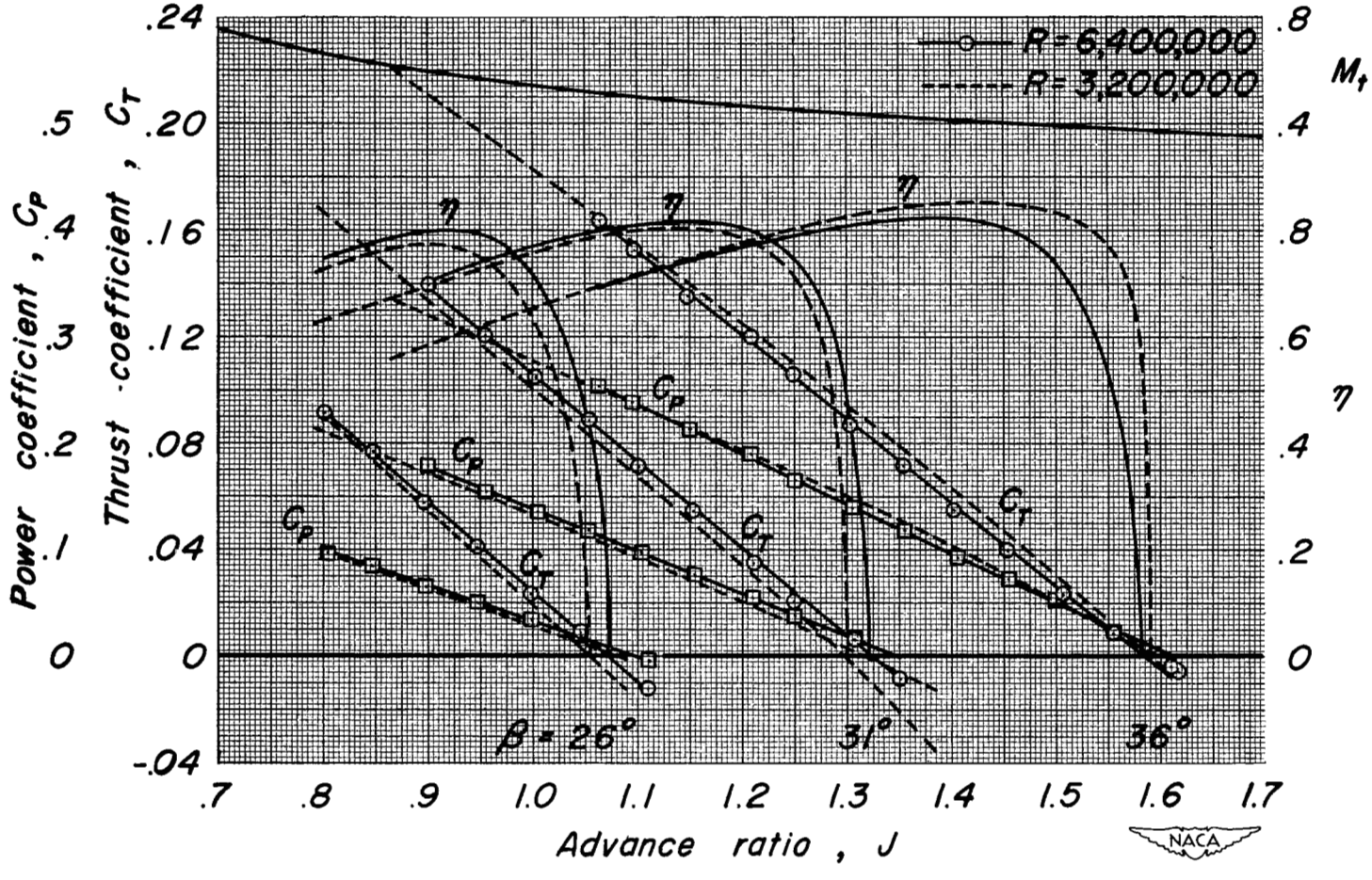

(b) M, 0.165

Figure 11.- Concluded.

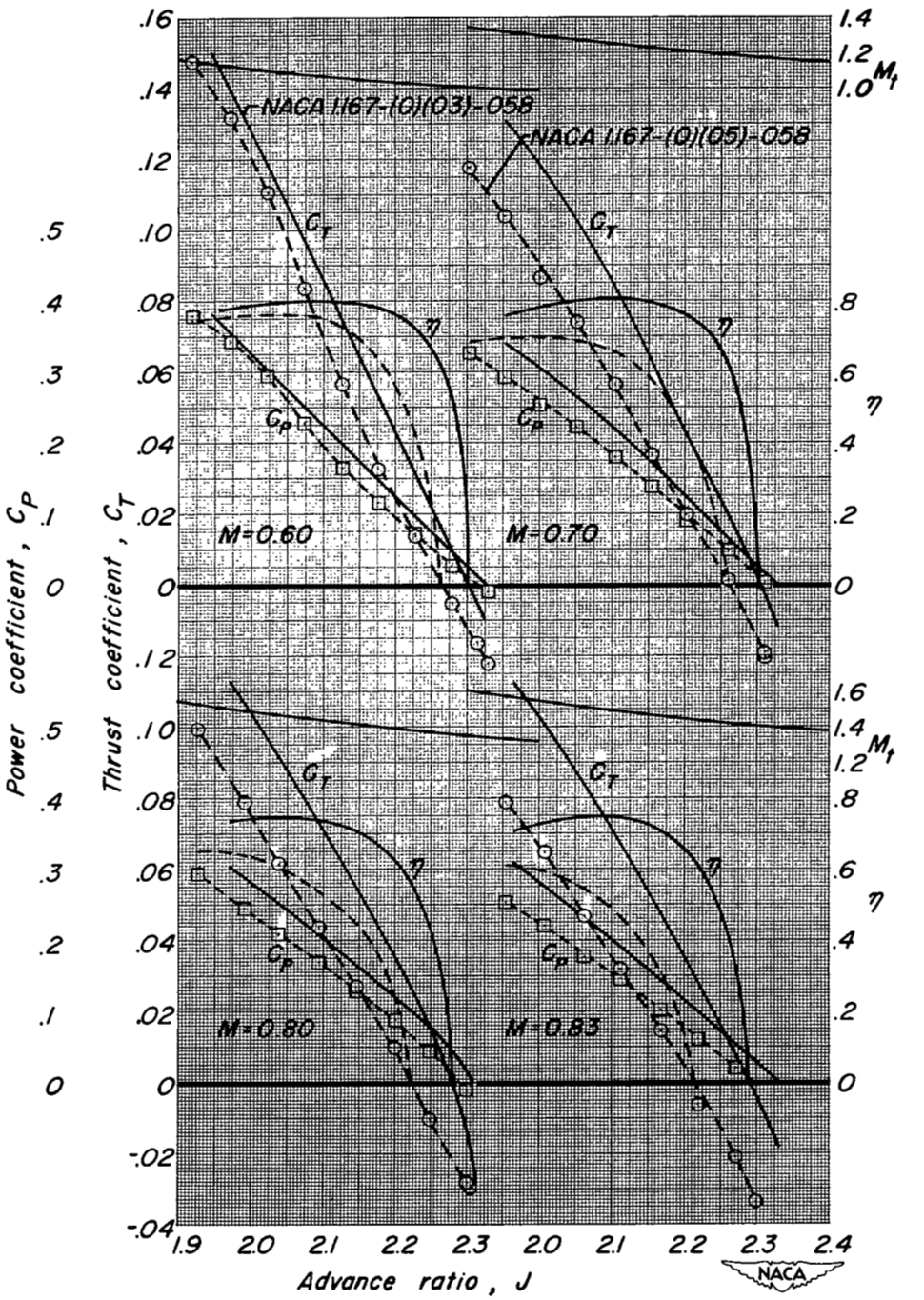

Figure 12.- Characteristics of the NACA 1.167-(0)(03)-058 and the NACA 1.167-(0)(05)-058 propellers at several Mach numbers; R, 1,600,000; β, 46°; α, 0°.

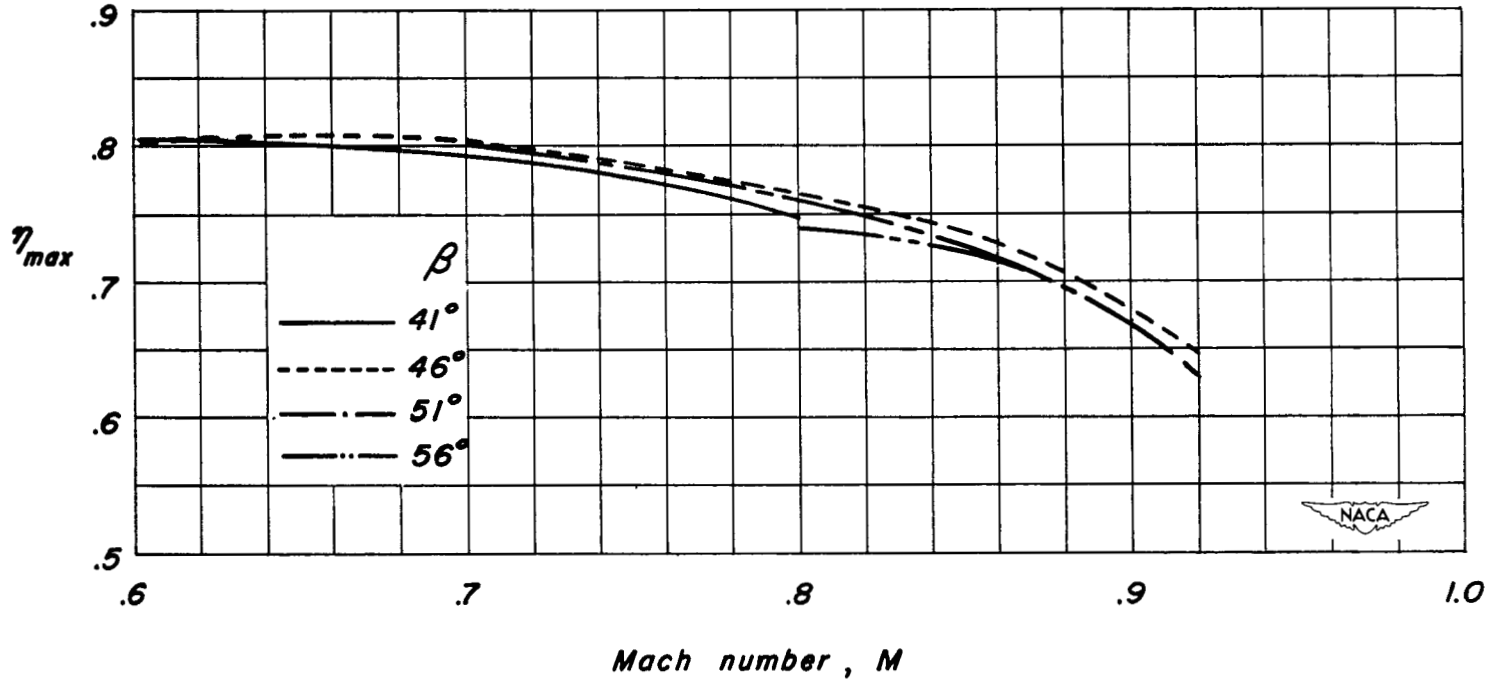

Figure 13.- The effect of forward Mach number on the maximum efficiency of the NACA 1.167-(0)(03)-058 propeller; R, 1,600,000; α, 0°.

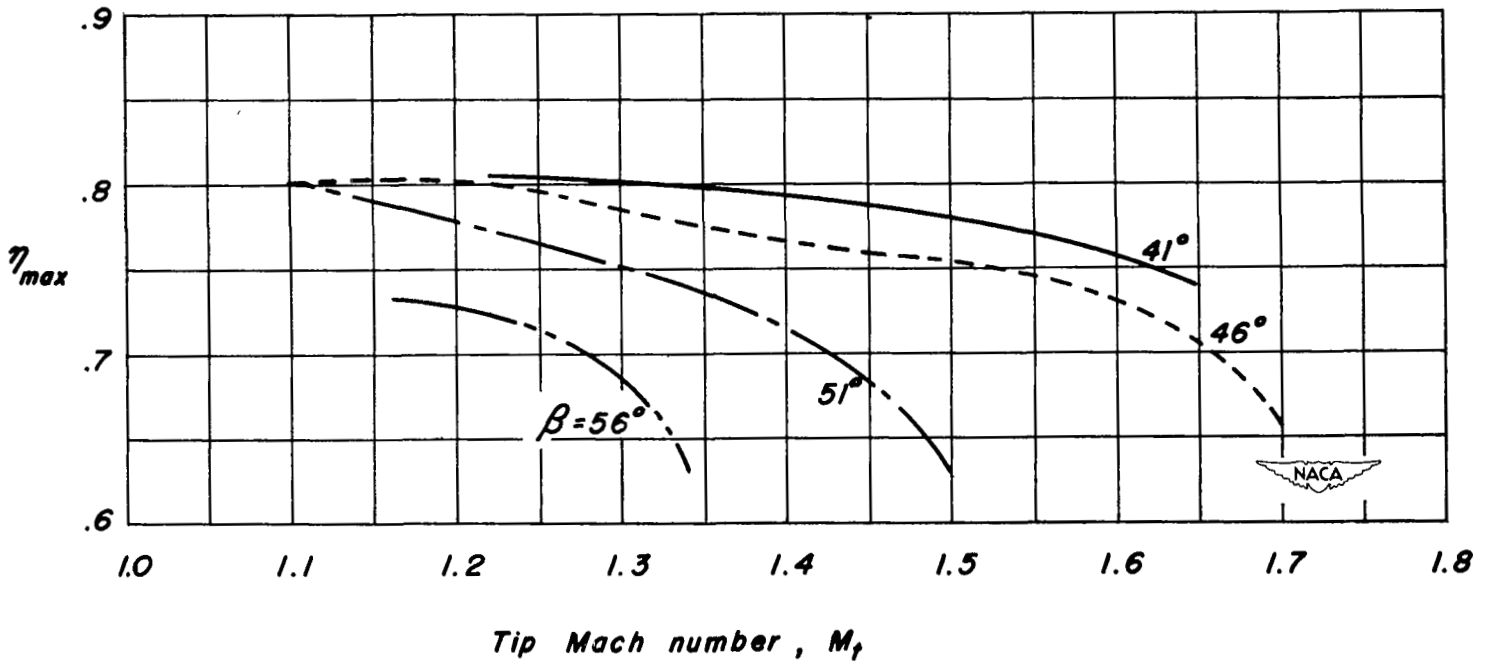

Figure 14.- The variation of maximum efficiency with tip Mach number for the NACA 1.167-(0)(03)-058 propeller; R, 1,600,000; α, 0°.

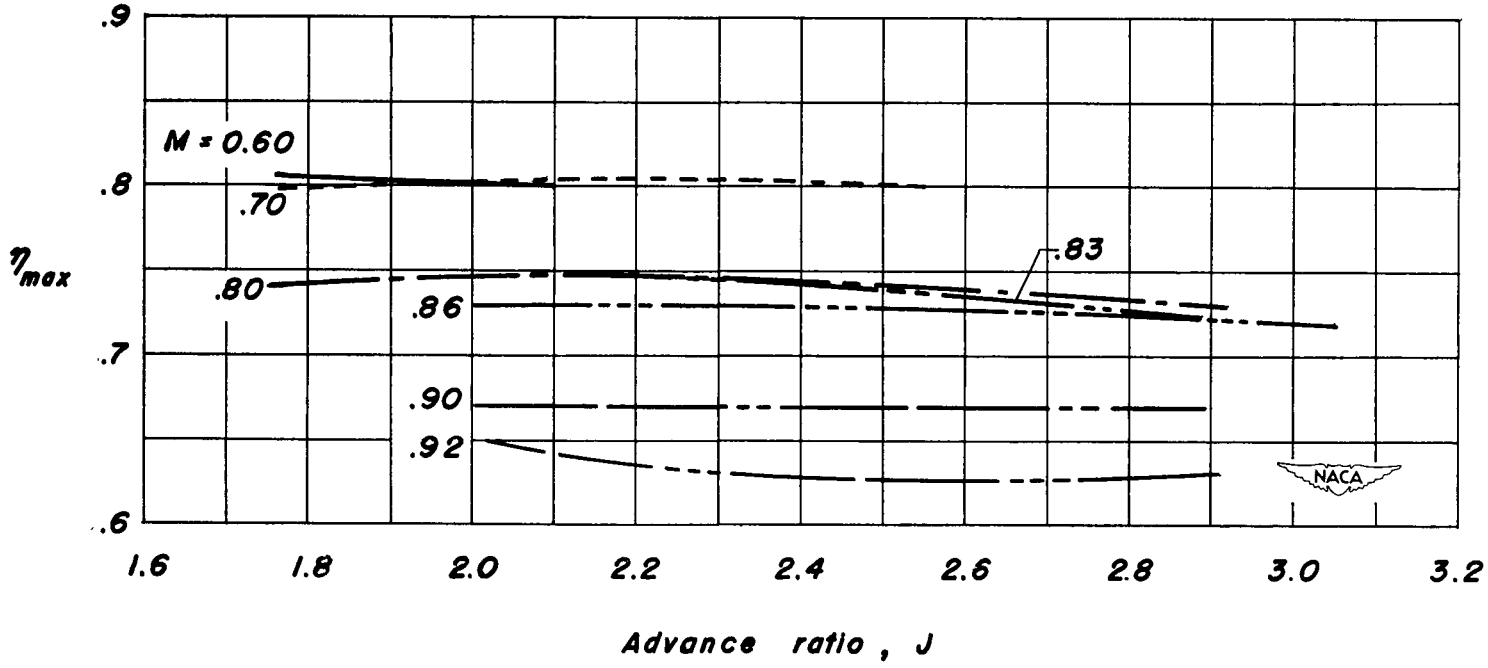

Figure 15.- The variation of maximum efficiency with advance ratio for the NACA 1.167-(0)(03)-058 propeller; R, 1,600,000; α, 0°.

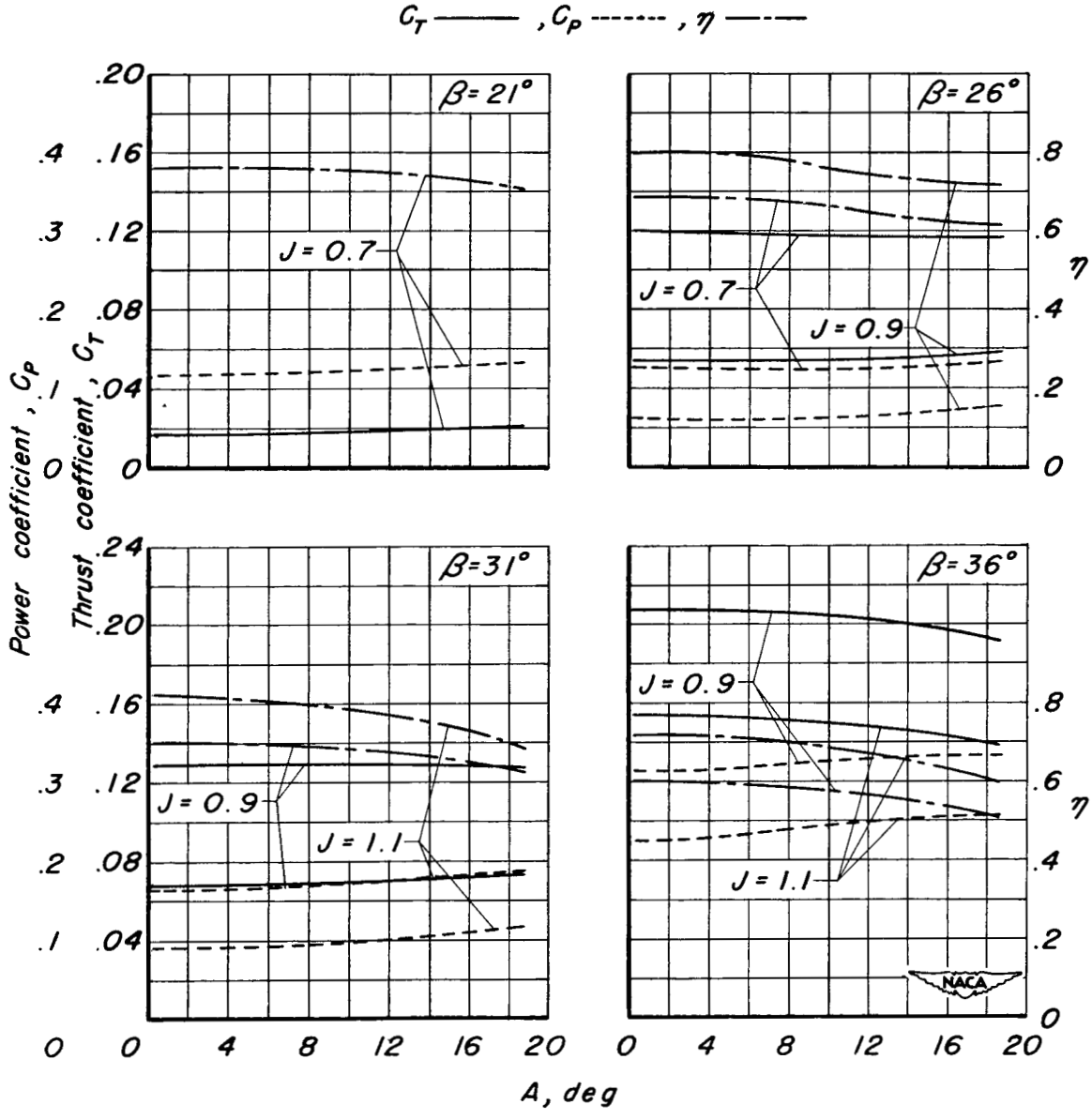

Figure 16.- The variation with stream inclination of thrust coefficient, power coefficient, and efficiency for the NACA 1.167-(0)(05)-058 propeller; R, 3,200,000; M, 0.123.

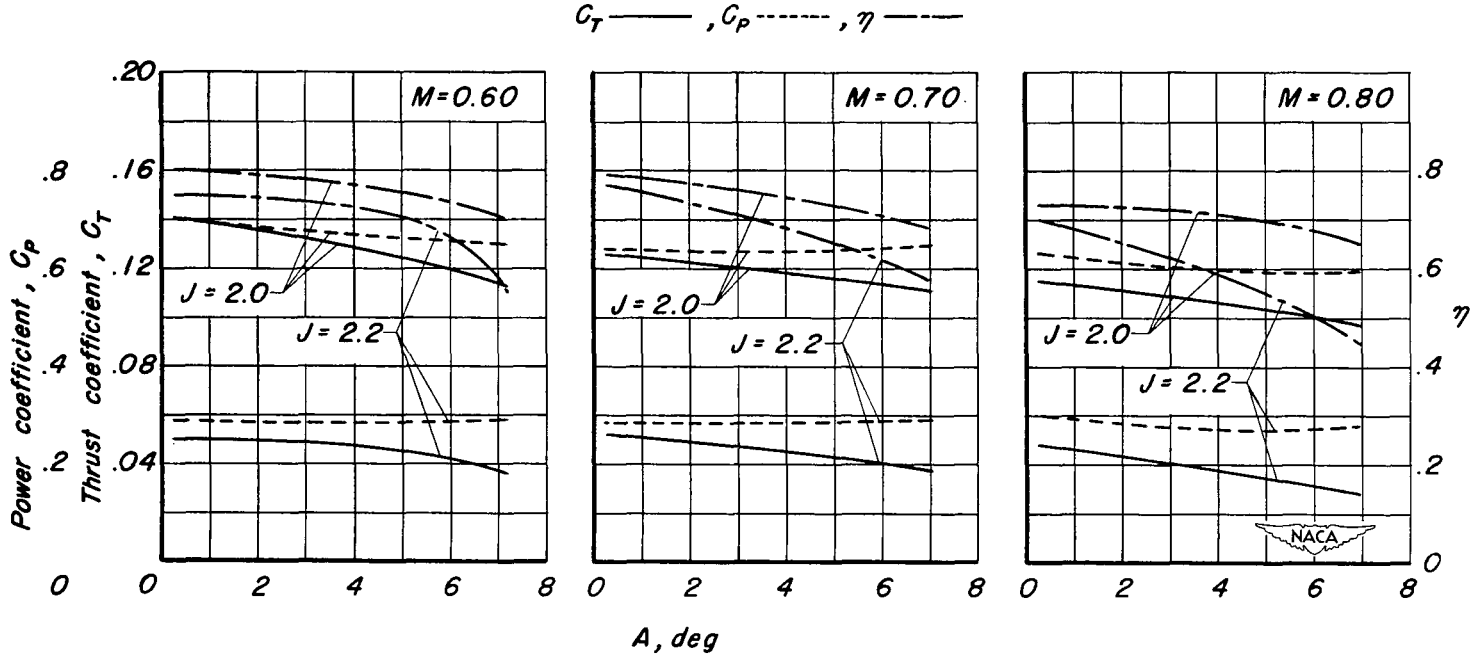

Figure 17.- The variation with stream inclination of thrust coefficient, power coefficient, and efficiency for the NACA 1.167-(0)(03)-058 propeller, R, 1,600,000; β, 46°.

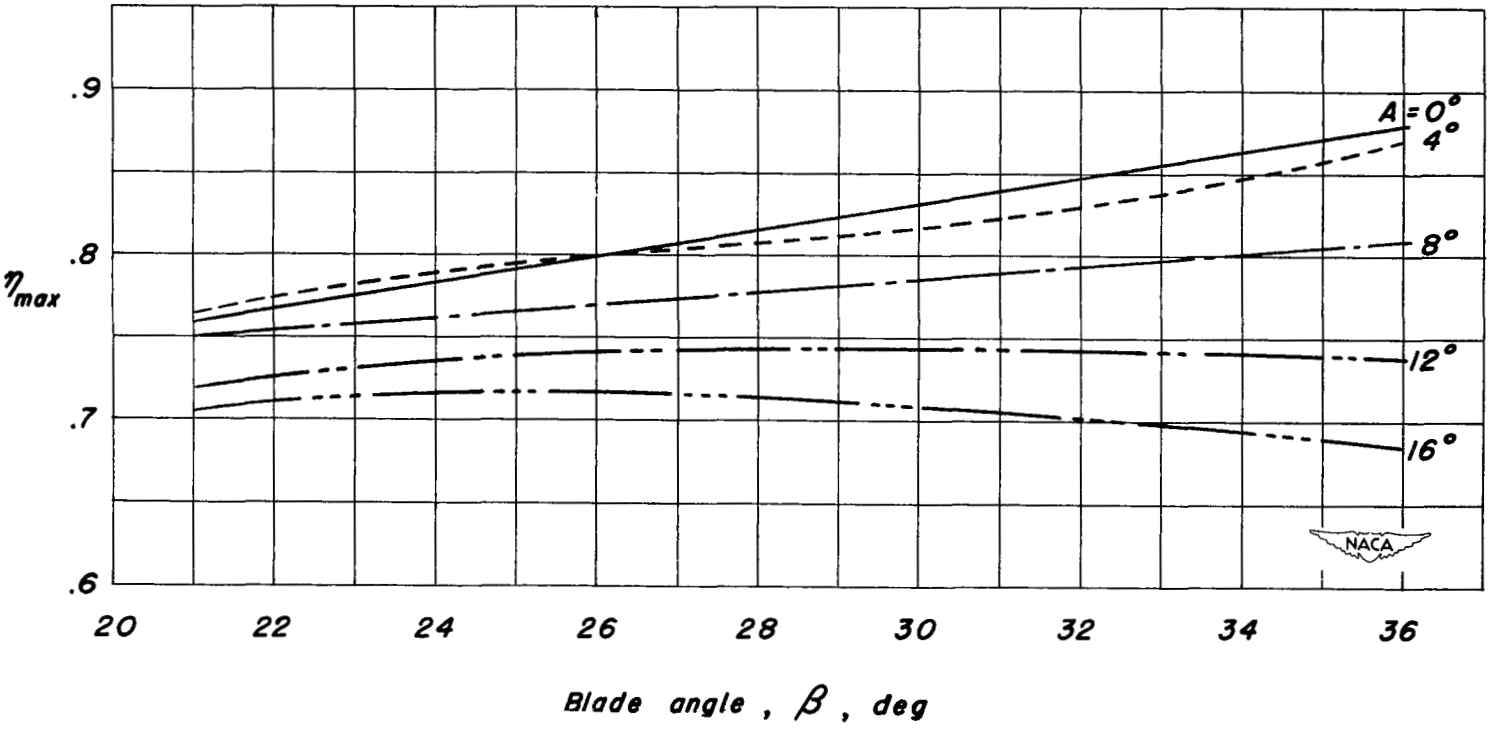

Figure 18.- The effect of blade angle and stream inclination on the maximum efficiency of the NACA 1.167-(0)(05)-058 propeller; R, 3,200,000; M, 0.123.

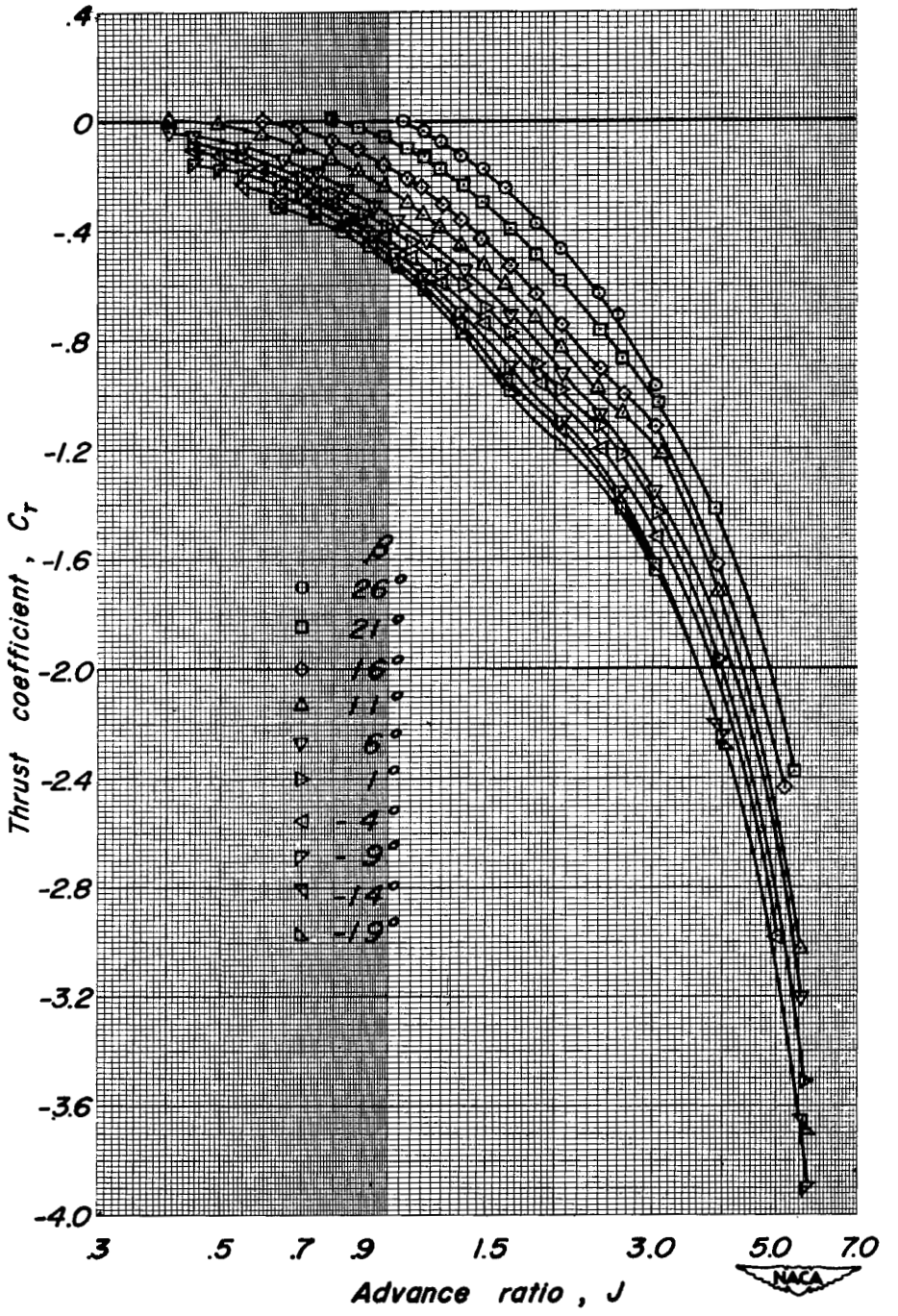

(a) C_T vs J

Figure 19.- Characteristics of the NACA 1.167-(0)(05)-058 propeller in negative thrust; R, 3,200,000; M, 0.082; α, 0°.

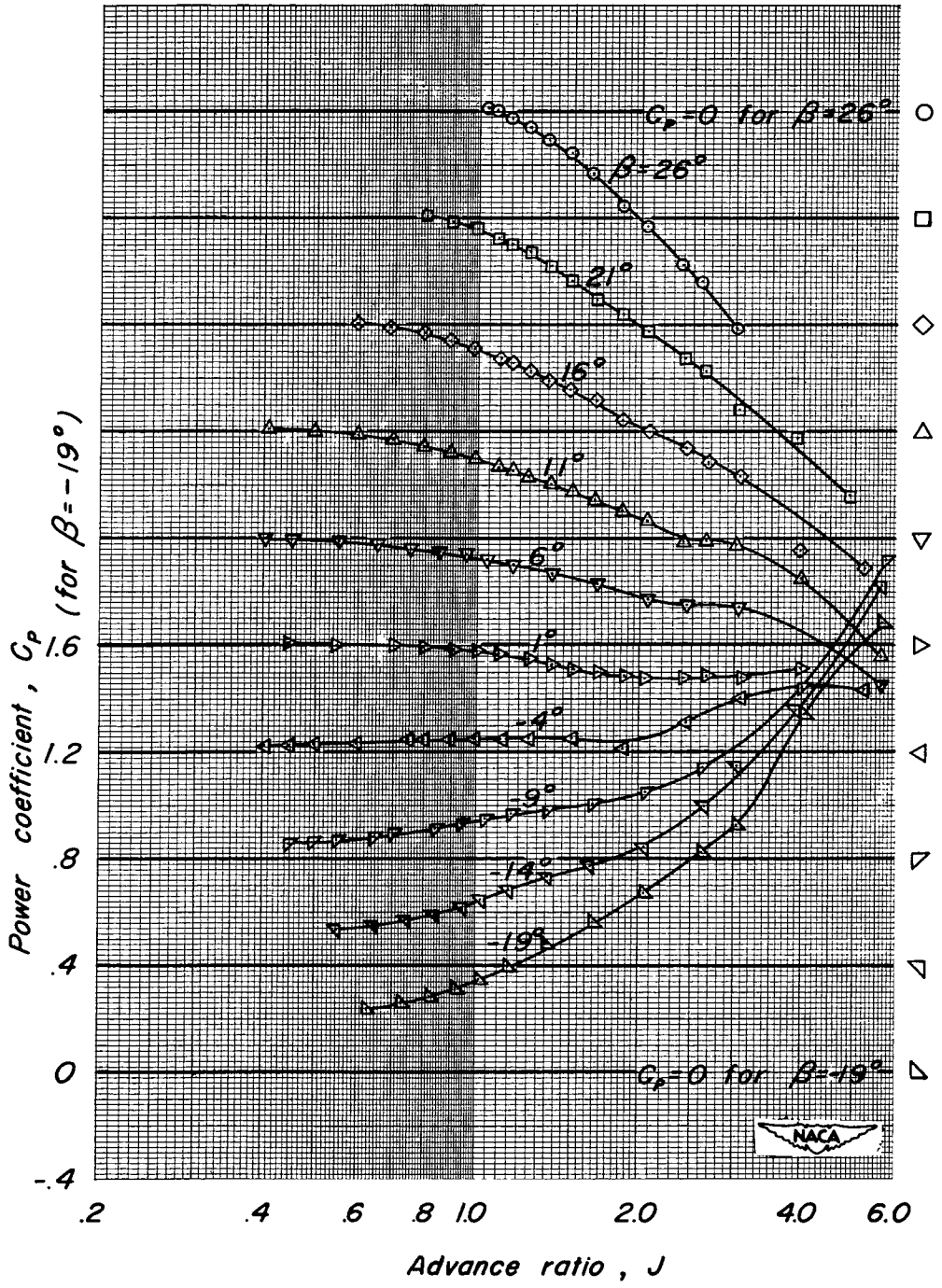

(b) C_p vs J

Figure 19.- Concluded.

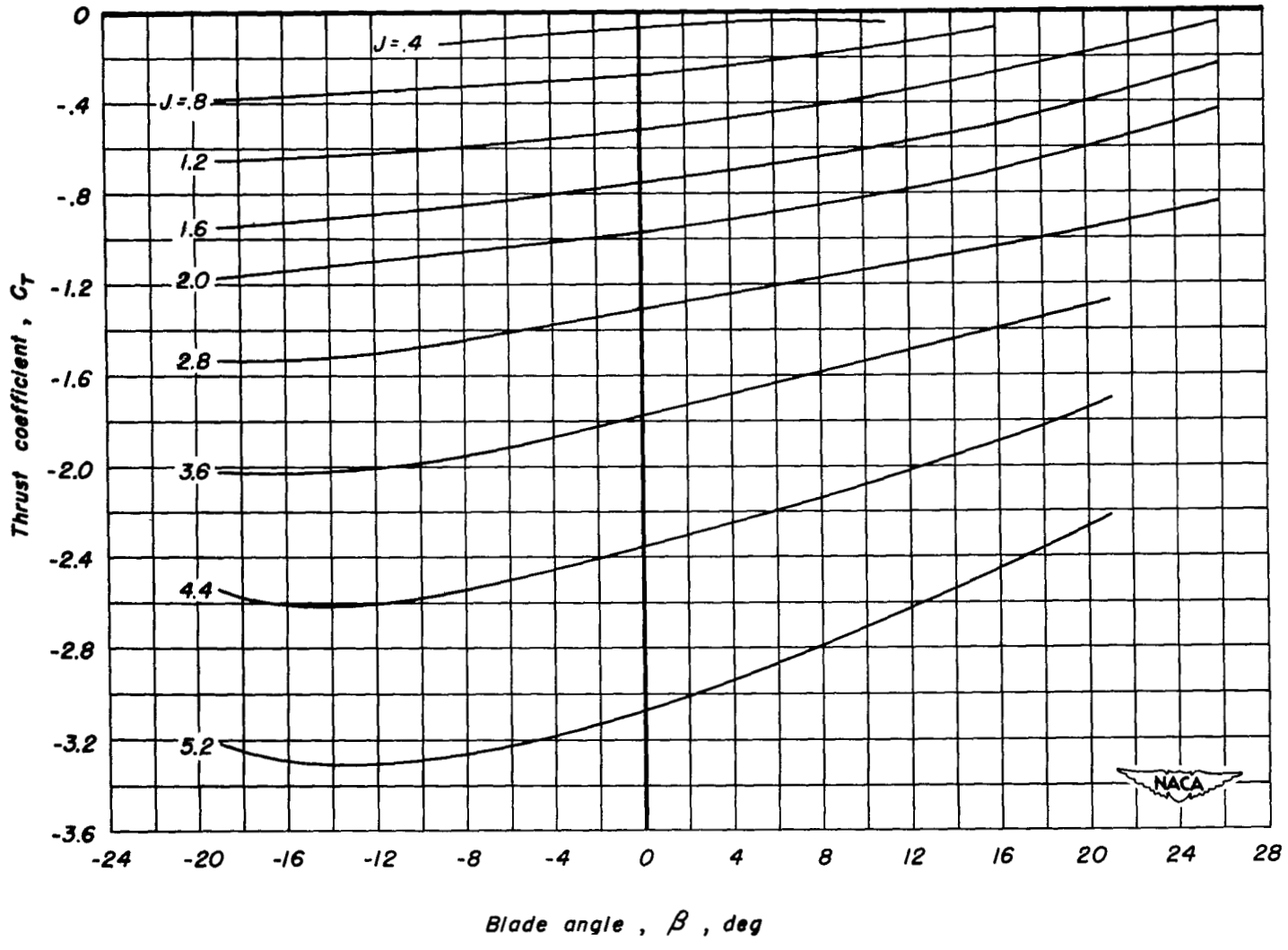

(a) C_T vs β

Figure 20.- The effect of blade angle on the characteristics of the NACA 1.167-(0)(05)-058 propeller in negative thrust; R, 3,200,000; M, 0.082; α, 0°.

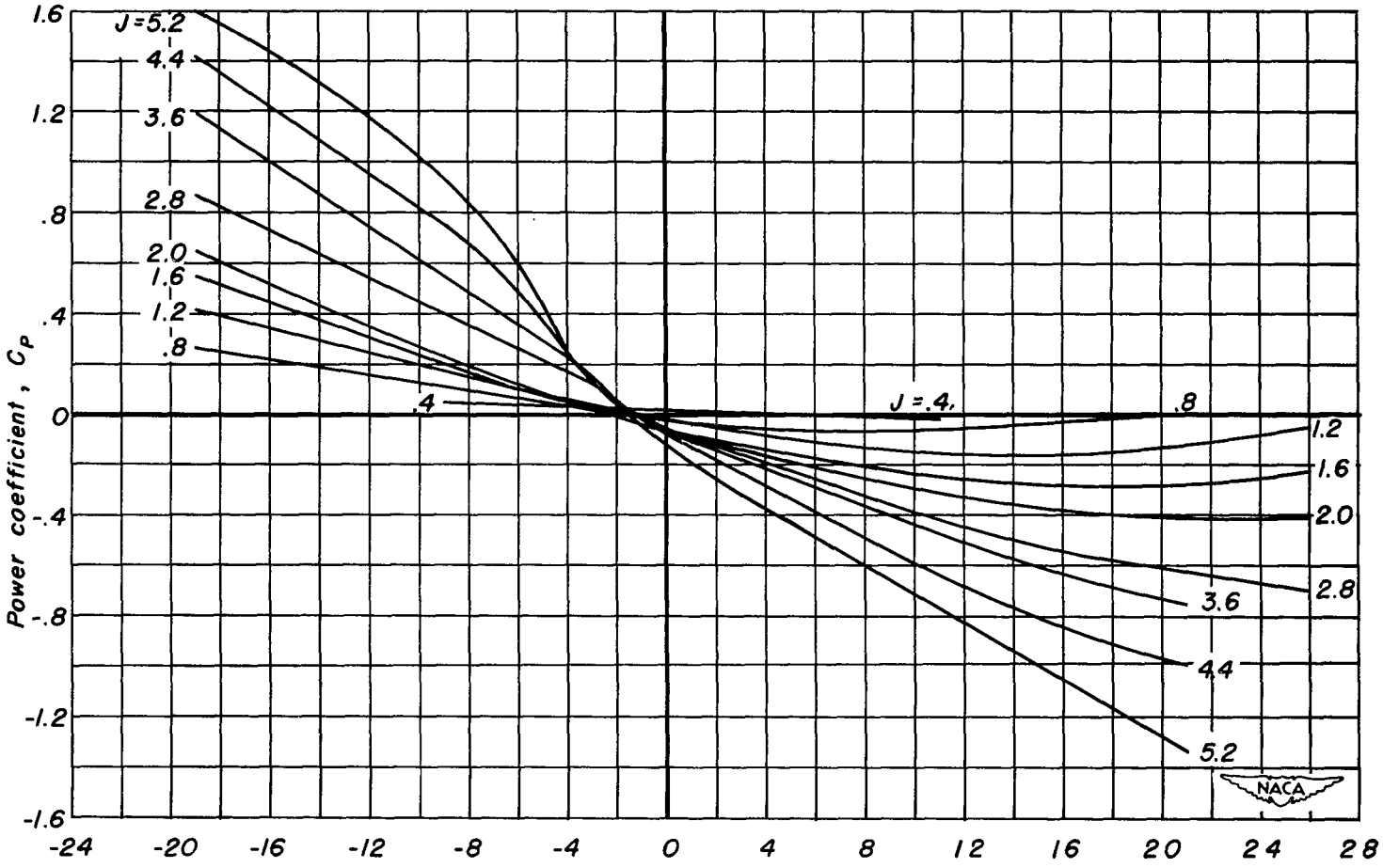

(b) C_P vs β

Figure 20.- Concluded.

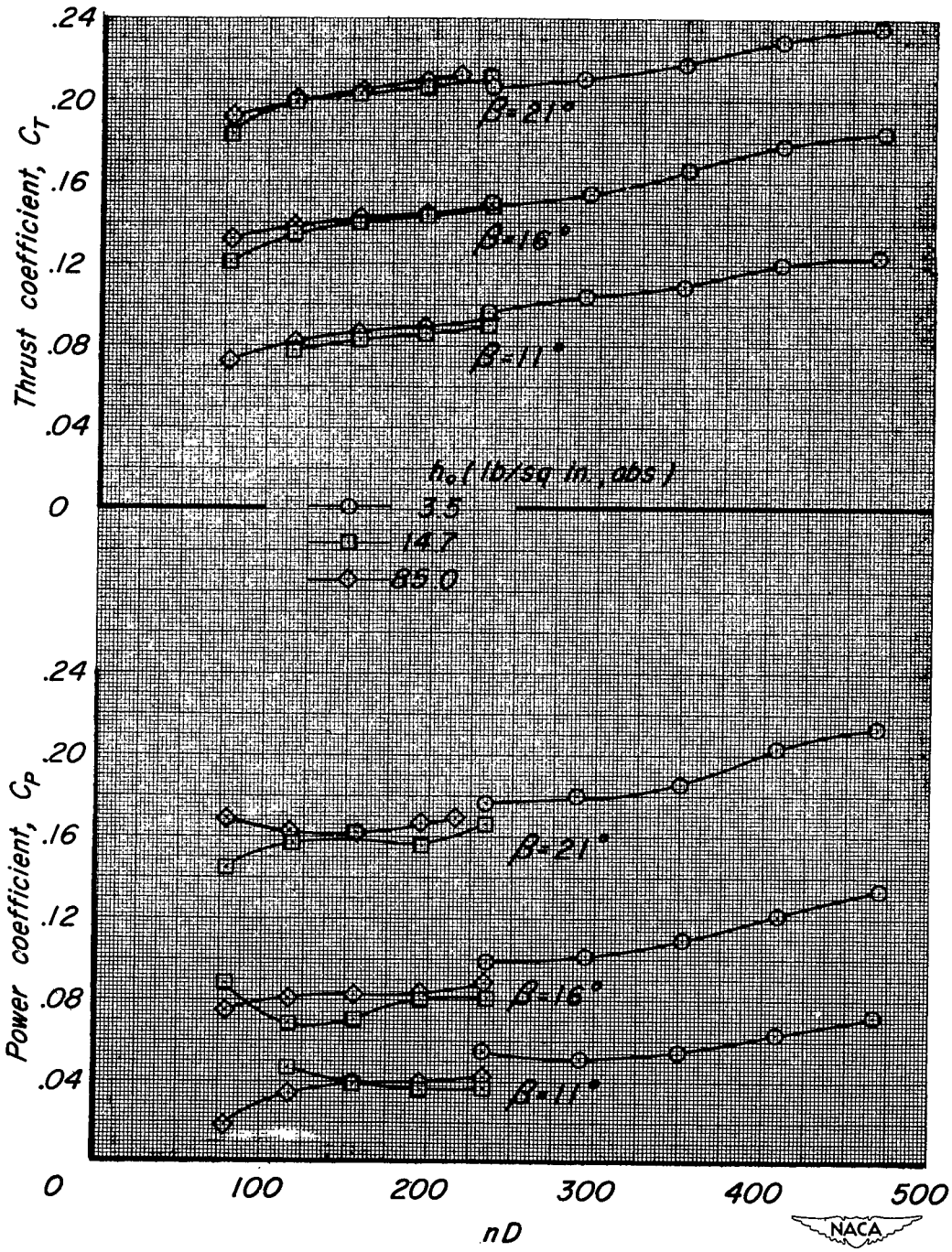

Figure 21.- Static thrust characteristics of the NACA 1.167-(0)(05)-058 propeller.

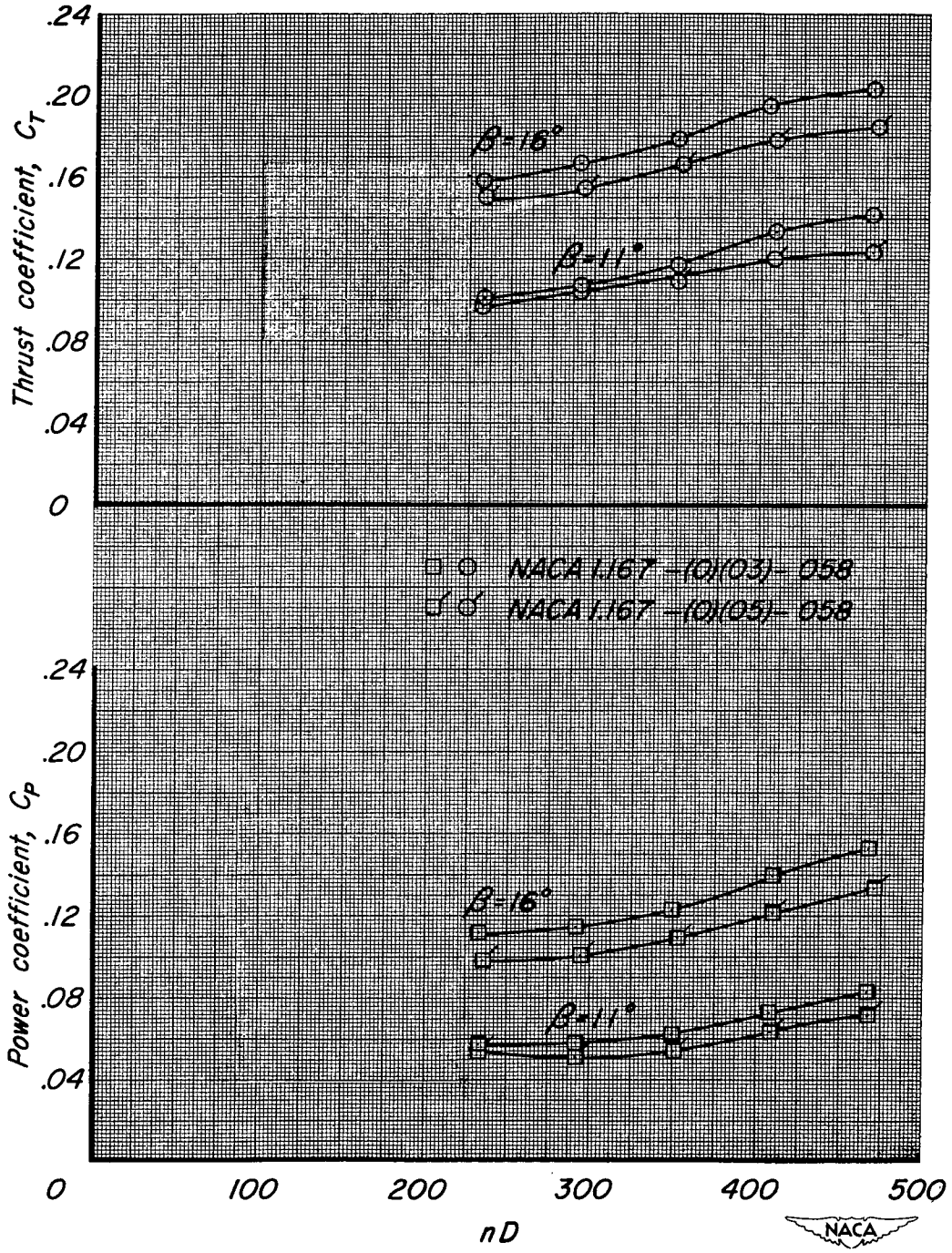

Figure 22.- Static-thrust characteristics of the NACA 1.167-(0)(03)-058 and the NACA 1.167-(0)(05)-058 propellers. Tunnel pressure, 3.5 pounds per square inch absolute.

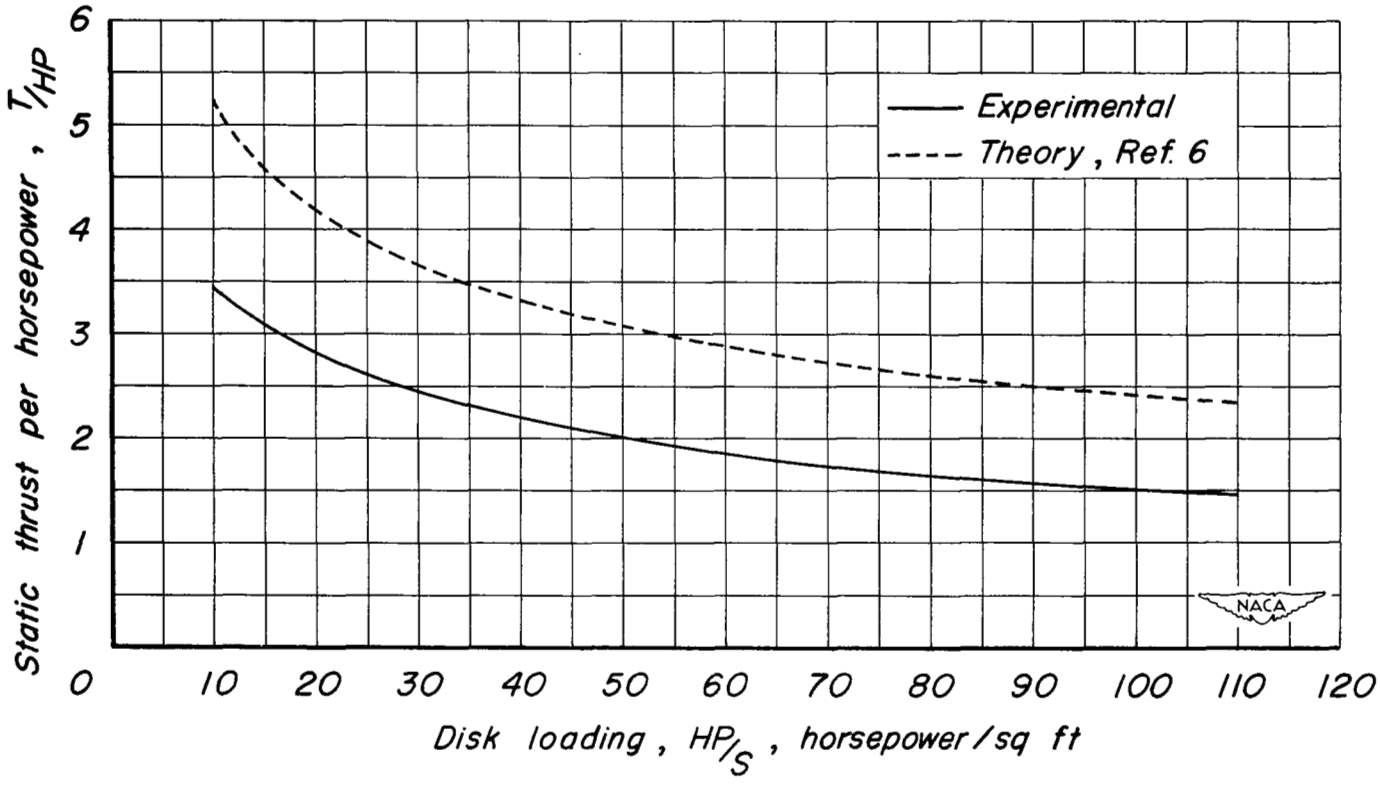

Figure 23.- Comparison with theory of the variation of sea level static thrust per horsepower with power disk loading for the NACA 1.167-(0)(05)-058 propeller.

NACA-Langley - 8-31-53 - 325

SECURITY INFORMATION